NTNU – Trondheim
Norwegian University of
Science and Technology

The use of Model Predictive Control and Distributed Battery Energy Storage Systems for Primary Frequency Control

Morten Rusten Hestdal

Master of Science in Cybernetics and Robotics
Submission date: June 2014
Supervisor: Lars Imsland, ITK

Norwegian University of Science and Technology
Department of Engineering Cybernetics

The use of Model Predictive Control and Distributed Battery Energy Storage Systems for Primary Frequency Control

Morten Rusten Hestdal

June 2014

Master of Science in Engineering Cybernetics
Department of Engineering Cybernetics
Norwegian University of Science and Technology

Supervisor 1: Professor Lars Imsland
Supervisor 2: Ole Jakob Sørdalen, Eltek AS

Abstract

As the worlds energy demand rises together with a global awareness over climate-changes due to burning of fossil fuel, and disasters due to accidents at nuclear power plants, the demand for renewable energy grows. The two most available sources for renewable energy are solar power and wind power. However, these energy sources are unreliable since they only produce power under certain weather conditions. Among other things, fluctuations in the grid frequency of 50Hz increases. Primary Frequency Control is part of the toolbox for frequency control. In order to deliver primary frequency control, a plant with a rectifier, an inverter, and a battery package is needed. Eltek is a power electronics company which delivers backup power solutions for sites with communication antennas or other communication equipment. This thesis will try to develop a control strategy which controls a number of sites used both for backup power and primary frequency control. This controller needs to follow the regulations given by the transmission system operator. The transmission system operator operates the power grid and is responsible for primary frequency control. However, private companies may also participate. This is done by auctions where several stakeholders make a bid for how much power can be delivered for a certain price. The winner of the bidding is allowed to deliver primary frequency control services for a certain time period.

In this thesis, the controller chosen is a model predictive controller. This is an optimizing control strategy, and the controller should distribute power limits to each site. These limits may be different for up-regulation of the frequency and down-regulation of the frequency, and they should be distributed in such a way that it minimizes the battery degradation. The models for battery degradation are too complex to be implemented in a model predictive controller, hence a simpler model is implemented which focuses on one part of battery degradation. The controller developed is simulated in a plant modelled in SIMULINK, which consists of 20 sites with different battery sizes. Each site is modelled after a site controller suggested by the danish transmission system operator Energinet.dk. Battery degradation models are also implemented at each site. One for lead-acid batteries and one for lithium-ion batteries. Half the sites uses lead-acid degradation model, and the rest uses the lithium-ion degradation model. These models are based on part physics part heuristics.

Sammendrag

Samtidig som verdens ernegibeghov stiger, øker den globale bevisstheten på klimaendringer som følge av forbrenning av fossilt brennstoff, og katastrofer med langvarige konsekvenser fra ulykker ved atomkraftverk. Dette fører til at etterspørselen etter bærekraftig fornybar energi vokser. De to mest tilgjengelige kildene for fornybar energi er solenergi og vindkraft, men disse energikildene er upålitelige, siden de bare produserer energi under visse værforhold. Dette kan føre til blant annet at avvik fra den nominelle nettfrekvensen i strømnettet på 50Hz kan skje oftere. Primærfrekvensregulering er et av verktøyene som blir brukt for å holde nettfrekvensen på 50Hz. For å kunne levere tjenesten primærfrekvensregulering, trengs det et anlegg med en likeretter, en vekselretter og en type energilagring. Denne oppgaven vil fokusere kun på batterier som energilager. Eltek er et kraftelektronikkselskap som leverer nødstrømsløsninger for telekommunikasjonsoperatører. Denne oppgaven vil gå ut på å utvikle en kontrollstrategi som styrer et distribuert nettverk av anlegg som både deltar i primærfrekvensregulering og leverer nødstrømsløsninger til kommunikasjonsutstyr. Denne kontrolleren må også sørge for at primærfrekvensregulering blir utført i tråd med de reguleringene som den lokale TSOen (selskapet som drifter strømnettet) har satt. TSOen er ansvarlig for å levere primærfrekvensregulering, men private selskaper kan også delta. Dette gjøres ved auksjoner der flere interessenter kommer med et bud på hvor mye effekt de kan levere i et visst tidsrom og til hvilken pris. Vinnerene av burdunden får lov til å levere primærfrekvensregulering i det tidsrommet der budet er akspetert.

I denne avhandlingen er en modellprediktiv kontrollstrategi valgt. Dette er en optimaliserende kontrollstrategi, og oppgaven til kontrolleren blir å distribuere effektgrenser ut til hvert anlegg. Disse grensene kan være forskjellig for opp- og nedregulering av frekvensen, og de bør være fordelt på en slik måte at batterislitasje blir minimalisert. Mange fysiske modeller for batterislitasje er for komplekse til å bli implementert i en modellprediktiv kontroller, så en enklere modell som fokuserer på en egenskap ved batterislitasje er brukt. Kontrolleren som er utviklet her simuleres i en modell av systemet i SIMULINK. Denne modellen består av 20 anlegg som er forskjellige størrelsesmessig. Hvert anlegg er modellert etter en kontroller som er utviklet av den danske TSOen Energinet.dk. Batterslitasjemodeller er også implementert på hvert anlegg. Det finnes

en modell for blybatterier, og en for litium-ion batterier. Halvparten av anleggene har blybatterier, mens resten har litium-ion batterier. Disse modellene er basert delvis på fysiske og delvis på statistiske modeller.

Preface

This thesis was written in the spring of 2014. The work was carried out for a Master's thesis written at the end of the Msc study program at the Department of Engineering Cybernetics at the Norwegian University of Science and Technology. The project was carried out in collaboration with the power electronics company Eltek, which also suggested the research topic of this thesis. I would like to thank my supervisor at the Department of Engineering Cybernetics, Professor Lars Imsland and my supervisor at Eltek, Ole Jakob Sørdalen for all the help and guidance I have received. I would also like to thank my fellow students for tips and tricks, and also moral support.

Trondheim, 2014-06-02

Morten Rusten Hestdal

Contents

List of Figures

Nomenclature

List of Acronyms

MPC Model Predictive Cotnrol

PFC Primary Frequency Control

SOC State of Charge

SOH State of Health

DOD Depth of Discharge

TSO Transmission System Operator

ESS Energy Storage System

BESS Battery Energy Storage System

CV Controlled Variable

MV Manipulated Variable

DV Disturbance Variable

EOL End of Life

List of Variables

Δf Frequency Deviation

H The sum of all inertias of the rotating masses in a grid

ΔP_m Change in generated power in a grid

ΔP_L Change in the load power in a grid

D Load damping coefficient of the grid

$P_{\mathbf{PFC}}$ Power supplied for PFC

$P_{\mathbf{min}}$ Maximum power output at maximum negative Δf

$P_{\mathbf{max}}$ Maximum power output at maximum positive Δf

$x_{\mathbf{SOC}}$ SOC of a BESS

$\Delta x_{\mathbf{SOC}}$ Change in SOC of a BESS

$\eta_{\mathbf{load}}$ Load efficiency of battery

$\eta_{\mathbf{gen}}$ Generating efficiency of battery

$u_{\mathbf{load}}$ Charge power of battery

$u_{\mathbf{gen}}$ Generating power of battery

$u_{\mathbf{net}}$ Sum of u_{load} and u_{gen}

$x_{\mathbf{DOD}}$ DOD in a BESS

$C_{\mathbf{deg,lithium}}$ Degradation in Lithium-ion battery

$\alpha_{\mathbf{cap}}$ Time varying parameter for battery time-wear

$\beta_{\mathbf{cap}}$ Time varying parameter for battery cycle-wear

Q Current throughput in degradation model for lithium ion

U Battery voltage

$C_{\mathbf{remaining}}$ Remaining capacity lead-acid battery

$C_d(0)$ Initial battery capacity lead-acid battery

$C_{\mathbf{deg,lead\text{-}acid}}$ Battery degradation lead-acid battery

$C_{\mathbf{deg,limit}}$ EOL battery capacity

c_z Fitted parameter degradation of lead-acid battery model

Z_W Weighted cycle count lead-acid degradation model

Z_N Nominal cycle count

Z_{IEC} Number of nominal cycles a battery can reach before EOL

I_{dch} Discharged current

C_N Nominal battery capacity lead-acid

f_{SOC} SOC stress factor lead-acid degradation model

$f_{\mathbf{acid}}$ Acid stress factor lead-acid degradation model

$f_{\mathbf{stratification}}$ Stratification stress factor degradation model

I_{10} The 10-hour current. The current which completely discharges a fully charged battery in 10 hours

I_{ref} Reference current f_{acid} model. Usually the 10-hour current

$f_{\mathbf{plus}}$ Increase in acid stratification

f_{minus} Decrease in acid stratification

$f_{minus,gassing}$ Decrease in acid stratification due to gassing

$f_{minus,diffusion}$ Decrease in acid stratification due to diffusion

$c_{\mathbf{plus}}$ Fitted parameter stratification model

$c_{\mathbf{minus}}$ Fitted parameter stratification model

$I_{\mathbf{gas}}$ Gassing current

$U_{\mathbf{gas,0}}$ Nominal voltage for gassing

$\_\mathbf{gas,0}$ Nominal temperature for gassing

$I_{\mathbf{gas,0}}$ Gassing current at $U_{\text{gas,0}}$ and $T_{\text{gas,0}}$

$D_{\mathbf{batt}}$ Diffusion constant for sulfuric acid

$c_{\mathbf{SOC,0}}$ Constant slope SOC factor

$c_{\mathbf{SOC,min}}$ Impact of min SOC on the SOC factor

f_I Current factor

n Number of bad recharges

T Temperature

$P_{\mathbf{cell}}$ u_{net} but for one battery cell

$P_{\mathbf{BESS}}$ u_{net} but for a BESS

$C_{\mathbf{cell,kWh}}$ Battery cell capacity kWh

$C_{\mathbf{BESS,kWh}}$ BESS capacity kWh

$I_{\mathbf{cell}}$ Battery cell current

$I_{\mathbf{BESS}}$ BESS current

$C_{\mathbf{cell,Ah}}$ Battery cell capacity Ah

$C_{\mathbf{BESS,Ah}}$ BESS capacity Ah

$K_{\mathbf{charge}}$ Control gain for SOC compensation controller

K Parameter that decides K_{charge}

i Site number

$P_{\mathbf{SOC,compensation}}$ SOC compensation power

$batterylevel_{\mathbf{ref}}$ Battery reference level at site i in kWh

$batterylevel(i)$ Battery level at site in kWh

$\mathbf{SOC_{ref}}$ Reference SOC

Z Binary vector with information of sites available for PFC

$P_{\mathbf{load}}$ Site load power

$u_{\mathbf{max}}$ Maximum Δf up-regulation for site i

$u_{\mathbf{min}}$ Maximum Δf down-regulation for site i

$I_{\mathbf{cap}}$ Inverter capacity

$R_{\mathbf{cap}}$ Rectifier capacity

$P_{\mathbf{ref,up}}$ Power that should be available for Δf up-regulation

$P_{\mathbf{ref,down}}$ Power that should be available for Δf down-regulation

SOC_{min} Lower bound on SOC

SOC_{max} Upper bound on SOC

$P_{\mathbf{slack,up}}$ Slack variable for Δf up-regulation in MPC2

$P_{\mathbf{slack,down}}$ Slack variable for Δf down-regulation in MPC2

$D_{\mathbf{cost}}$ Battery cycle cost

$N_{\mathbf{cycles}}$ Number of cycles in battery

ρ Battery price per kWh

Chapter 1

Introduction

1.1 Background

Today's power generation is mainly consisting of fossil fuel power plants, nuclear power plants and hydro power plants. The power output from these are very stable due to the nature of the energy sources(Thorbergsson et al., 2013). However, since fossil fuel power plants and nuclear power plants may have serious impacts on the environment ,and the world's supply of petroleum and radioactive materials is limited, a conversion to other energy sources is necessary in the near future. Hydro power plants are depending on waterfalls, and because of this hydro power alone cannot replace all the energy from fossil fuelled and nuclear powered plants. Hence, other renewable energy sources are required. The two largest renewable energy sources aside from hydro power are wind power and solar power(Thorbergsson et al., 2013). However, the energy output from these plants can be unpredictable since they only produce power in certain weather conditions. This causes instabilities in the grid, and one implication of these instabilities is variations in the grid frequency. This phenomena is present in the grid already, but it increases with the amount of renewable energy sources installed in the grid. Even today some countries have a lot of these energy sources installed such as Germany where more than $17GW$ of solar photovoltaic was installed as early as 2010(Heussen et al., 2012). Denmark already have a lot of installed wind power, and in March 2012 it was decided in the Danish Parliament that 50% of the electric power supply should

consists of wind-power by 2020 (Thorbergsson et al., 2013). They also plan to have a carbon-free society by 2050. As a consequence of these goals, the grid characteristics will change and create new both known and unknown challenges.

To face these challenges that this change in the grid will create, Energy Storage Systems are proposed. ESSs might serve several different applications such as peak shaving, schedule compliance, Integration of Distributed Generation and Primary Frequency Control. (Koller et al., 2013). Of these applications, primary frequency control was found to be the most profitable, at least in the Danish energy market (Thorbergsson et al., 2013). Several energy storage systems might be considered for primary frequency control, including super capacitors, flywheels, compressed air and pumped hydro. However, battery energy storage system (BESS) are chosen because they are very easy to scale (Koller et al., 2013), and the technology have been improved in the latter years due to their necessity in hybrid and electrical vehicles.

It is the local transmission system operator (TSO) that has the responsibility of maintaining the correct grid frequency by implementing frequency controllers. These can be divided in to three levels of controllers, namely primary, secondary and tertiary frequency control (Thorbergsson et al., 2013). The focus in this paper will be on primary frequency control (PFC) which is the one of the three with the smallest response time but also the smallest energy storage. The PFC market works in such a way that the TSO auctions out intervals where the operators that contributes in the market offers to enable a certain amount of power for a certain amount of money. The winner of the auction gets to deliver the service in one specific interval. In Denmark 2013, there is an auction every 24 hour which auctions out 4 hour long intervals (Thorbergsson et al., 2013). Different operators can participate in the same interval. To be an operator, the PFC plants needs to follow some regulations which will be explained in detail later in the paper. The operator gets paid by the TSO just for making the power available, not for the amount of power actually used for PFC. The infrastructure needed for this is a site with an inverter, a rectifier and some kind of energy storage.

Eltek is a company which delivers backup power solutions for telecommunication companies. The telecommunication companies have sites with some kind of communication equipment, battery pack for backup power and power electronics delivered by Eltek. The power electronics is usually a rectifier, however, inverters are considered in-

stalled such that the telecommunication companies might participate in a PFC market. Eltek also produces a centralized site-surveillance system with a two-way communication such that it is able to both receive and send information to each site.

1.2 Opportunity and Challenge

In the new proposed regulations for PFC from the danish TSO (Energinet.dk, 2013), a PFC site consists of

- BESS
- Rectifier/inverter
- Site controller which controls the power through the rectifier/inverter.

In addition to this, Eltek's sites includes a communication load. In order to minimize battery wear, a centralized Model Predictive Controller (MPC) is suggested. This controller would use the battery level on each site and estimations of the power consumption to calculate an optimal set of maximum and minimum limits for each site controller. In other words, decide how much power each site should contribute with for PFC.
Some extra conditions:

- Some batteries are lead-acid batteries which prefer to be fully charged.
- Some batteries are lithium-ion, and they prefer to be half-charged. However, since these batteries also will be used for backup power for the communication load, only half of the stored energy are available for PFC, hence the set poin for these batteries needs to be higher than 50% and is therefore chosen to be 70%.
- Some sites only have rectifiers, while some sites have inverters with different capacities than the rectifier on the site.
- The rectifiers and inverters have a maximum power throughput at 8kW.
- The communication between the centralized MPC and the sites are slow, such that the sites only gets and update from the MPC every 10th second.

- The quantities that are measured are the battery voltage, battery current and the current through the rectifier/inverter.

1.3 Project tasks

- Describe the state of the art
- Describe the business case. What should be minimized by the MPC in order to maximize profit?
- From the description of the business case and physical constraints, suggest objectives of the MPC together with a control structure.
- Implement a test environment in MATLAB/Simulink.
- Implement an MPC controller in MATLAB/Simulink.
- Test the suggested MPC against another, more naive solution.
- Run tests with real data.

1.4 State of the Art

Controlling energy storages is done in a large scale, and the use of MPC for controlling these have also been explored. For example, the use of MPC for controlling a BESS for smoothing the output of a wind farm (Teleke et al., 2010),(Khalid and Savkin, 2010). However, these approaches controls only one site each, and uses an objective function in the MPC which tries to minimize the difference between the BESSs power output and a reference power. Another approach to control a BESS has also been explored, where the goal of the objective function is to minimize the square of the cycle depth, the deviation in battery level from a reference battery level and a factor that punishes the controller for using high powers(Koller et al., 2013). However, it is still only explored for a single site. There are also done a lot of research on battery degradation modeling in the latter years, especially for battery models that are partly based on physics and then fitted to statistical models (Schiffer et al., 2006),(Schmalstieg et al., 2014). These models

combines the speed of heuristic models, and the accuracy of physical models. State of health (SOH) prediction is important in electric and hybrid electric vehicles, which is a growing market. Some of the SOH models uses state-space models and extended kalman filters for the prediction.

1.5 Approach

There are two controllers developed in this thesis. One, which is the main controller called MPC2, and a reference controller which uses a naive approach to distribute the power between the sites. Both controllers should give limits to a set of PFC sites as output. MPC2 should distribute the power in such a way that the batteries experience the same cycle depths, while MPC1 choose the distribution more or less on a random basis. However, both controllers should make sure the battery levels on each site does not exceed fully charged, or below a certain lower limit. Another approach was also suggested, where instead of the MPC giving a set of limits as output, a set of biases added to the power-flow into the battery was given instead. However, this approach was scrapped on an early stage because of the fact that the MPCs should have a sample time of 10 seconds, and if the frequency changes during this 10 second period, which it is likely to do, there is a risk of delivering power to the grid without having to deliver power to the grid.

1.6 Outline

The report starts in chapter 2 with explaining the background theory used to implement the SIMULINK model. This includes the battery degradation models, an explanation of PFC, and the discrete time models used in the MPCs prediction, and also a brief introduction of MPC. Then comes chapter 3 where the implementations in SIMULINK are explained. It starts with the explanation of the control hierarchy, and an overview of the system, before the implementation of the site controlellers and battery degradation models are presented. Then the business case is explained, before it ends with a presentation of the two MPCs. In chapter 4 the results are presented, and they are discussed in chapter 5. Then the conclusion comes in chapter 6. Appendix A includes the MATLAB

code used in the SIMULINK models, and Appendix B consists of additional plots, where all the plots from a simulation is included.

Chapter 2

Background Theory

This chapter contains the background theory used in this project. Subsections 2.1, 2.2, 2.3, 2.5, 2.6 are partially based on the work done in the project thesis (Hestdal, 2013). It starts with an explanation of PFC, then it presents two battery properties, which are state of charge and depth of discharge. These properties might be defined differently elsewhere, but the definitions here are preferred because they are designed with an MPC controller in mind (Koller et al., 2013). The battery degradation section is divided into two parts, where one is about one specific type of lithium-ion battery, and the other is a model of the degradation of a specific lead-acid type battery. There is also a corrosion part in the lead-acid model, but this is neglected in the implementation because, in conversations with a professor in chemistry, it was considered to be very complex and not very crucial for the performance of the model. These models are only used in the plant-replacement model because implementing them in the MPC is considered to be very complex in comparison to the improvement in the solutions from the MPC. At the end there is a brief presentation of a linear-MPC and a short explanation of the optimization toolbobx for MATLAB, YALMIP.

2.1 Primary Frequency Control

Deviations from the nominal frequency in power grids occur because of imbalance between the power generated by the power plants and the power consumed by the con-

sumers. Primary frequency control (PFC) is a tool for helping the transmission system operator keeping the frequency at the nominal value which is 50Hz in Europe. Including PFC, there are three different levels of frequency regulation where the two others are secondary frequency control and tertiary frequency control. The difference between the three are the reaction time and amount of energy stored. PFC are the fastest of the three, but a smaller amount of stored energy is required. This make batteries a well suited energy storage system for this service. The reason PFC is implemented is that the deviation from the nominal frequency, Δf, is depending on the power generated and consumed in the grid, and it follows this equation from (Ersdal et al., 2013)

$$\frac{d\Delta f}{dt} = \frac{1}{2H}(\Delta P_m - \Delta P_L) - \frac{D}{2H}\Delta f \tag{2.1}$$

Where ΔP_m is the total power produced from the three levels of frequency control combined, while ΔP_L represents the power imbalance in the grid. H is a constant which are the sum of the inertia of all the rotating masses. This implies that in a larger grid with many generators, H will be larger than for a small grid, hence the frequency is more stable. D is the load damping coefficient of the grid.

The power output from the ESS depends on Δf and should follow the curve in figure 2.1. The equation for this curve, which is implemented in the SIMULINK model, is:

$$P_{\text{PFC}} = \begin{cases} -\frac{\Delta f P_{\min}}{0.2}, & 0 \leq \Delta f < 0.2 \\ -\frac{\Delta f P_{\max}}{0.2}, & -0.2 < \Delta f \leq 0 \\ P_{\max}, & \Delta f \leq -0.2 \\ -P_{\min}, & \Delta f \geq 0.2 \end{cases} \tag{2.2}$$

However, some slack is allowed as mentioned in (Energinet.dk, 2013). The regulations from the danish TSO, the accuracy of the frequency measurement must be better than 10mHz, which means a hysteresis of 20mHz around 0Hz is allowed. The resolution of the frequency measurement must be at least 1mHz, and the delay from the measurement to the correct power output from the site is given is maximum 2 seconds. The danish TSO, Energinet.dk has made an acceptance test which every plant must manage. This is explained in detail in the results section.

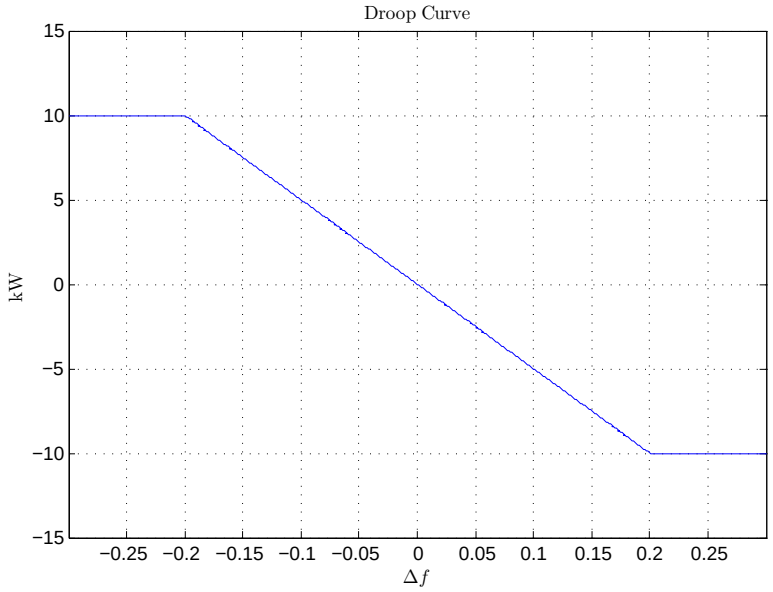

Figure 2.1: Example of droop curve with maximum power output $10kW$

2.2 Battery State of Charge

State of charge (SOC) is a normalized measure of the stored energy in a battery. The following discrete time equation for the change in SOC can be found in (Koller et al., 2013).

$$\Delta x_{\text{SOC}}(k+1) = \eta_{\text{load}} u_{\text{load}}(k) - \eta_{\text{gen}}^{-1} u_{\text{gen}}(k) - v(k) \tag{2.3a}$$

$$0 \leq \eta_{\text{load}} \leq 1 \tag{2.3b}$$

$$0 \leq \eta_{\text{gen}} \leq 1 \tag{2.3c}$$

In this equation, u_{load} is the charge power and u_{gen} is the discharge power. η_{load} and η_{gen} is the charge/discharge efficiency. Since a battery can not be charged and discharged at the same time, either u_{load} or u_{gen} must be zero. $v(k)$ is a stationary energy loss from the battery, and is ignored in the rest of the paper. Assuming no energy

loss in the batteries, using this piecewise defined equation for u_{net}, u_{net} becomes the energy flow in/out from the battery. If u_{net} is positive, then the battery is charging, and if it is negative, the battery is discharging.

$$u_{\text{net}} = \begin{cases} u_{\text{load}}, & u_{\text{load}} \geq 0 \\ -u_{\text{gen}}, & u_{\text{gen}} \geq 0 \end{cases} \tag{2.4}$$

This is the same as

$$u_{\text{net}} = u_{\text{load}} - u_{\text{gen}} \tag{2.5}$$

Then, $\Delta x_{\text{SOC}}(k+1)$ may be written as

$$\Delta x_{\text{SOC}}(k+1) = u_{\text{net}}(k) \tag{2.6}$$

2.3 Battery Depth of Discharge

Depth of discharge is a measure which is defined in several ways in literature (Koller et al., 2013). The one used in this paper is a vector where the first element grows when the battery is charging, and the second element grows when the battery is discharging. In the transition from charging to discharing and vice versa, both elements of the vector is reset to zero. The model in equation 2.7 is taken from (Koller et al., 2013). By minimizing the number and depth of battery cylces, battery lifetime should be improved.

$$x_{\text{DOD}}(k+1) = \begin{cases} A_d x_{\text{DOD}}(k) + a_c \Delta x_{\text{SOC}}, & u_{\text{net}} > 0 \\ A_d x_{\text{DOD}}(k) - a_d \Delta x_{\text{SOC}}, & u_{\text{net}} < 0 \\ a_i, & u_{\text{net}} = 0 \end{cases} \tag{2.7a}$$

$$A_c = \begin{bmatrix} 1 & 0 \\ 0 & 0 \end{bmatrix}, \qquad A_d = \begin{bmatrix} 0 & 0 \\ 0 & 1 \end{bmatrix} \tag{2.7b}$$

$$a_c = \begin{pmatrix} 1 \\ 0 \end{pmatrix}, \qquad a_d = \begin{pmatrix} 0 \\ 1 \end{pmatrix}, \qquad a_i = \begin{pmatrix} 0 \\ 0 \end{pmatrix} \tag{2.7c}$$

SOC	0	0.1	0.2	0.3	0.5	0.6	0.7	0.8	0.85	0.9	0.95	1
V [V]	3.331	3.494	3.578	3.626	3.699	3.782	3.869	3.964	4.018	4.072	4.117	4.162

Table 2.1: The relationship between voltage and SOC

2.4 Battery Degradation

There are four major factors which causes battery degradation. These are temperature, charge power, state of charge and depth of discharge. These factors are the same both for lithium-ion batteries and lead-acid batteries. However, the models on how these factors effects the batteries are different for the two. The two models used in this thesis are based on part physics and part heuristics. This is to reduce runtime but still get accurate enough models.

2.4.1 Degradation of Lithium-Ion Batteries

This model of degradaton of lihtium-ion batteries were chosen because it is easy to implement, and contains models for the voltage. It also takes cycle depth into account. This model is made for a (Li(NiMnCo)O_2 based 18650 lithium-ion battery. The equation used in this thesis for change in capacity of lithium-ion batteries are taken from (Schmalstieg et al., 2014). The capacity fade model is dependent on the cell voltage, the quadratic average voltage, cycle depth, temperature and time.

$$C = 1 - \alpha_{\text{cap}} t^{0.75} - \beta_{\text{cap}} \sqrt{Q} \tag{2.8a}$$

Where Q is the current throughput in Ah, t is the time in days and β_{cap} and α_{cap} are parameters.

Table 2.4.1 that shows how the voltage changes with the sate of charge is given in (Ecker et al., 2013) which is also referred to by the article where the degradation model can be found. To be able to use this table in the degradation model, a continuous function $V = f(\text{SOC})$ is necessary. This was created by using a curve fitting tool in MATLAB called lsqcurvefit which takes table 2.4.1 and an nth order polynomial as input and fits the function to the data. The MATLAB script which does this is:

```
%Declaring the nth order polynomial. x(i) are the coefficients ...
    which are to be
%fitted to the voltage model, and x_data is the state of charge.
F = @(x,x_data) x(1)*x_data + x(2)*x_data.^2 + x(3)*x_data.^3 + ...
    x(4) + x(5)*x_data.^4;

%Initial values for the coefficients. The resulting theta will be ...
    theta =
%[x(1) x(2) x(3) x(4)]
theta01  = [1 1 1 1 1];

%State of charge
 XDATA = [0 0.1 0.2 0.3 0.5 0.6 0.7 0.8 0.85 0.9 0.95 1];

 %The voltage data
 YDATA = [3.331 3.494 3.578 3.626 3.699 3.782 3.869 3.964 4.018 ...
     4.072 4.117 4.162];

 %calls the MATLAB function lsqcurvefit
 [theta, resnorm,~,exitflag,output] = ...
     lsqcurvefit(F,theta01,XDATA,YDATA);
```

The resulting 4th order polynomial is:

$$U = 3.3324 + 2.1021soc - 5.8485soc^2 + 8.0326soc^3 - 3.4599soc^4 \tag{2.9}$$

The β_{cap} parameter is calculated from this equation:

$$\beta_{\text{cap}} = 7.348 \cdot 10^{-3} \cdot (ØV - 3.667)^2 - 7 \cdot 10^{-4} + 4.081 \cdot 10^{-3} \cdot \Delta DOD \tag{2.10}$$

Where the first term is a constant times the quadratic average voltage ($ØV$) minus the voltage 3.667, which is the voltage at SOC = 50%. The second term is a constant and the last term a constant multiplied with the cycle depth. Hence, β_{cap} accounts for both deviation from SOC = 50% and the depth of discharge. There is a difference in how DOD is defined in eq. (2.10) and eq. (2.7). ΔDOD from eq. (2.10) is the same as the DOD from eq. (2.7). The parameter α_{cap} is dependent on the cell voltage and the temperature and is calculated by this equation:

$$\alpha_{\text{cap}} = (7.543 \cdot V - 23.75) \cdot 10^6 \cdot e^{-\frac{6976}{T}} \tag{2.11a}$$

Where V is the cell voltage in volts and T is the cell temperature in kelvins.

2.4.2 Degradation of Lead-Acid Batteries

The model of degradation of lead-acid batteries are taken from (Schiffer et al., 2006), and it is made for. One simplification that has been made that differs from the original article is that the capacity loss from corrosion is neglected. The equation for the total capacity loss then only depends on the battery degradation.

$$C_{\text{remaining}} = C_d(0) - C_{\text{deg}}(t) \tag{2.12}$$

Where $C_{\text{remaining}}$ is the remaining capacity, $C_d(0)$ is the initial capacity and $C_{\text{deg}}(t)$ is the capacity loss due to degradation. This is given by:

$$C_{\text{deg}} = C_{\text{deg,limit}} e^{-c_z(1-(Z_W(t)/1.6Z_{\text{IEC}}))} \tag{2.13}$$

$C_{\text{deg,limit}}$ is the end of lifetime capacity usually about 80% of the original capacity. c_z is a fitted parameter equal to 5. Z_W is a weighted cycle count, and Z_{IEC} is the maximum number of cycles under normal operating conditions. The number of nominal cycles is calculated this way(C_N is the nominal battery capacity of 54Ah):

$$Z_N = \int_0^t \frac{|I_{\text{dch}}(\tau)|}{C_N} d\tau \tag{2.14}$$

However, in the lifetime calculations executed in this thesis, a weighted number of cycles is used:

$$Z_W(t) = \frac{1}{C_N} \int_0^t |I_{\text{dch}}(\tau)| f_{SOC}(\tau) f_{\text{acid}}(\tau) d\tau \tag{2.15}$$

The f_{SOC} factor takes state of charge into account, and f_{acid} is a factor that counts the effect that acid stratification has on the battery degradation. This phenomenon is that the concentration of the acid differs in the top of the battery and the bottom. (str).

The light concentration in the top of the battery enhances corrosion of the plates, and the higher concentration in the bottom speeds up sulfation on the plates lower in the battery. It also makes the state of charge seem higher than it really is. There are three ways to reverse this effect. These are tipping the battery, rest the battery (diffusion) and overcharging the battery such that gases are created by the electrodes to stir the acid. Oxygen are then created by the cathode, and hydrogen by the anode. This process is called electrolysis. The equations that describes these phenomena are:

$$f_{\text{acid}} = 1 + f_{\text{stratification}} \sqrt{\frac{I_{\text{ref}}}{|I|}} \tag{2.16a}$$

$$f_{\text{stratification}} = \int (f_{\text{plus}} - f_{\text{minus}})\, dt, f_{\text{stratification}} \geq 0 \tag{2.16b}$$

$$f_{\text{plus}}(t) = c_{\text{plus}}(1 - SOC_{\text{min}}|_{t_0}^{t}) e^{-3 f_{\text{stratification}}(t)} \frac{I_{\text{dch}}(t)}{I_{\text{ref}}} \tag{2.16c}$$

$$f_{\text{minus}} = f_{\text{minus,gassing}} + f_{\text{minus,diffusion}} \tag{2.16d}$$

$$f_{\text{minus,gassing}} = c_{\text{minus}} \sqrt{\frac{100Ah}{C_N}} \frac{I_{\text{gas,0}}(t)}{I_{\text{gas,0}}} e^{c_u (U_{\text{cell}} - U_{\text{ref}}) + c_T (T - T_{\text{gas,0}})} \tag{2.16e}$$

$$f_{\text{minus,diffusion}} = \frac{8 D_{\text{batt}}}{z^2} f_{\text{stratification}} 2^{T - 20^o C)/10K} \tag{2.16f}$$

I_{ref} is a normalized reference current for the current factor, $SOC_{\text{min}}|_{t_0}^{t}$ is the lowest SOC since the last full charge, t_0 is the time of the last full charge, t is the current time, c_{minus} and c_{plus} are fitted parameters, $I_{\text{gas,0}}$ is the normalized gassing current at $U_{\text{gas,0}}$ and $T_{\text{gas,0}}$, $I_{\text{gas, 0}}(t)$ is the actual gassing current. I_{ref} is the reference current, I_{dch} is the discharged current throughput, c_u is a voltage coefficient, c_T is a temperature coefficient, U_{cell} is the cell voltage, U_{ref} is a reference voltage for decreasing stratification, $T_{\text{gas,0}}$ is the nominal temperature for gassing, D_{batt} is the diffusion constant for the acid in the battery, and z is the height of the battery.

The stress factor for the SOC is calculated by this equation:

$$f_{\text{SOC}}(t) = 1 + (c_{\text{SOC,0}} + c_{\text{SOC,min}}(1 - SOC_{\text{min}}(t)|_{t_0}^{t})) \times f_I(I, n) \Delta t_{\text{SOC}}(t) \tag{2.17}$$

Parameter	C_N	Z_{IEC}	U_0	ρ_c	ρ_d	C_d	I_{ref}	z	$I_{\text{gas},0}$	c_u	c_T
Value	54Ah	600	2.1V	0.42	0.699	1.75	-5.4A	20cm	20mA	$11V^{-1}$	$0.06K^{-1}$
Parameter	$U_{\text{gas},0}$	$T_{\text{gas},0}$	$c_{\text{SOC},0}$	$c_{\text{SOC,min}}$	SOC_{limit}	SOC_{ref}	c_{plus}	c_{minus}	U_{ref}	D_{batt}	
Value	2.23V	298K	$6.614\times10^{-5}h^{-1}$	$3.307\times10^{-3}h^{-1}$	0.90	0.95	1/30	0.1	2.5	$20\times10^{-9}m^2s^{-1}$	

Table 2.2: Parameters used in the lead-acid degradation model

The current factor $f_I(I,n)$ is equal to:

$$f_I(I,n) = \sqrt{\frac{I_{\text{ref}}}{I}}\sqrt[3]{\exp(+\frac{n}{3.6})} \tag{2.18}$$

n is a number that increases for each bad recharge, meaning every time the SOC reaches the fully charged state. A continuous model for n is:

$$\Delta n = \frac{0.0025 - (SOC_{\text{ref}} - SOC_{\text{max}})^2}{0.0025} \tag{2.19}$$

The gassing current, which is the portion of the current used for electrolysis is given by this equation:

$$I_{\text{gas}}(t) = \frac{C_N}{100Ah} I_{\text{gas},0} e^{(c_u(U-U_{\text{gas},0})+c_T(T-T_{\text{gas},0}))} \tag{2.20}$$

2.5 Model Predictive Control

MPC is an optimizing control strategy where the goal is to minimize some objective function subject to some physical constraints and limitations over a certain time horizon. For each step, it takes some input, which are called the Controlled Variables (CVs), and calculates what the optimal output for each time-step over the prediction horizon must be in order to minimize the objective function. The output of an MPC is often called Manipulated Variables (MVs). It then picks the MVs at t = 1 and sends it to the process. If the objective function is a convex function and the constraints consists of linear equalities and box-constraints such as in equation 2.21, the resulting optimization problem to be solved in each step will be a convex optimization problem which is easy and fast to solve (Foss and Heirung, 2013).

$$x^{\text{low}} \leq x_i \leq x^{\text{high}} \tag{2.21}$$

$$\min_z f(z) = \sum_{t=0}^{N-1} \frac{1}{2} x_{t+1}^T Q_{t+1} x_{t+1} + d_{x,t+1} x_{t+1} + \frac{1}{2} u_t^T R_t u_t + d_{u,y} + \frac{1}{2} \Delta u_t^T R_t \Delta u_t^T + s_t P \tag{2.22a}$$

$$\text{s.t.} \tag{2.22b}$$

$$x_{t+1} = A_t + B_t u_t \tag{2.22c}$$

$$x_0 = \text{given} \tag{2.22d}$$

$$x^{\text{low}} \leq x_t \leq x^{\text{high}} + s \tag{2.22e}$$

$$u^{\text{low}} \leq u_t \leq u^{\text{high}} \tag{2.22f}$$

$$-\Delta u^{\text{high}} \leq \Delta u_t \leq \Delta u^{\text{high}} \tag{2.22g}$$

$$s \geq 0 \tag{2.22h}$$

$$Q_t \succeq 0 \tag{2.22i}$$

$$R_t \succeq 0 \tag{2.22j}$$

$$\Delta u_t = u_{t+1} - u_t \tag{2.22k}$$

$$z = \begin{bmatrix} x \\ u \end{bmatrix} \tag{2.22l}$$

In eq. (2.22), A_t and B_t are the discrete time system matrices, while Q and R are positive semi-definite weight matrices. This model can be found in (Foss and Heirung, 2013). In addition to CVs and MVs, there are also exists disturbance variables (DVs). These might be predicted in the model equations, they can be measured or ignored. If they are ignored, they should either be impossible to measure/predict or insignificant to the solution of the optimization problem. Slack variables may also be added, as in eq. (2.22e). This might be used if there is a chance that the plant may break its constraints. It may be implemented on both lower and upper box-constraints. It is also added to the objective function. This makes eq. (2.22e) a soft constraint. This means that if the plant breaks it constraints, the MPC will still be able to find a solution to the optimization problem. However, the weight on the slack variable in the objective function must be so high that the first priority is to minimize s. If a hard constraint is broken, such as in eq. (2.22f), the MPC cannot find a solution. However, hard constraints

are usually physical constraints which cannot be broken.

2.6 YALMIP

YALMIP is an optimization toolbox for MATLAB which makes it easy to implement. It is run by making a controller object which is made with the optimizer command. This call may look like this:

```
1
2 Controller = ...
      optimizer(constraints,objectives,sdpsettings('solver','gurobi'),
3 {[Controller inputs]},{[controller outputs]}
```

Where constraints contains all the constraints of the optimization problem, objectives contains the objective function, the vector with controller inputs may include the current state of the system (CVs), and the current disturbances (DVs). The controller output is the vector that contains the MVs.

Constraints and objectives can be defined like this:

```
1  %The prediction horizon:
2  L = 30;
3
4  %declare decision variables:
5  x = sdpvar(repmat(L,1,1),repmat(1,1,1));
6  u = sdpvar(repmat(L,1,1),repmat(1,1,1));
7
8  %declare constants
9
10 a = 0.5;
11 Q = 1;
12
13 objective = 0;
14 constraints = []
15 for k = 1:L
16
17     objective = objective + x(k)*Q*x(k)
```

```
18
19      constraints = [constraints, x{k+1} == x{k} + a*u{k}];
20      constraints = [constraints, 0 <= x{k} <= 1];
21  end
```

More detailed information about YALMIP may be found at (Löfberg, 2013).

Chapter 3

Methodology

This chapter is about the actual implementation of the system. First, the control hierachy is explained, and then an overview of the entire system is shown, before the implementation of the sites and degradation model is presented. At last, the site controller and the two MPC approaches are explained.

3.1 Control Hierarchy

The control hierarchy consists of four layers. The top layer is the decision making of the operator/TSO which makes an agreement that states how much power the overall system should deliver. The operator is the plant operator, the company that delivers the PFC service. This information is then sent down to the MPC layer in figure 3.1, which also receives the CVs from the plant. The MPC layer uses this information to calculate the optimal bounds (MVs) for each site and sends these down to the site controller layer. The site controller then uses the scheme in figure 3.5 and 3.6 to calculate the actual power throughput which is given directly to the plant. Figure 3.2 shows a more superficial representation of the information flow of the system for a system with n sites.

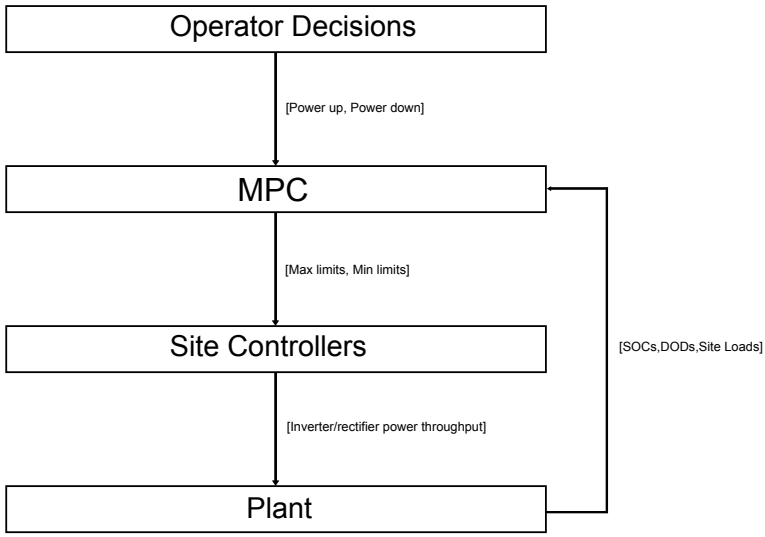

Figure 3.1: Control Hierarchy

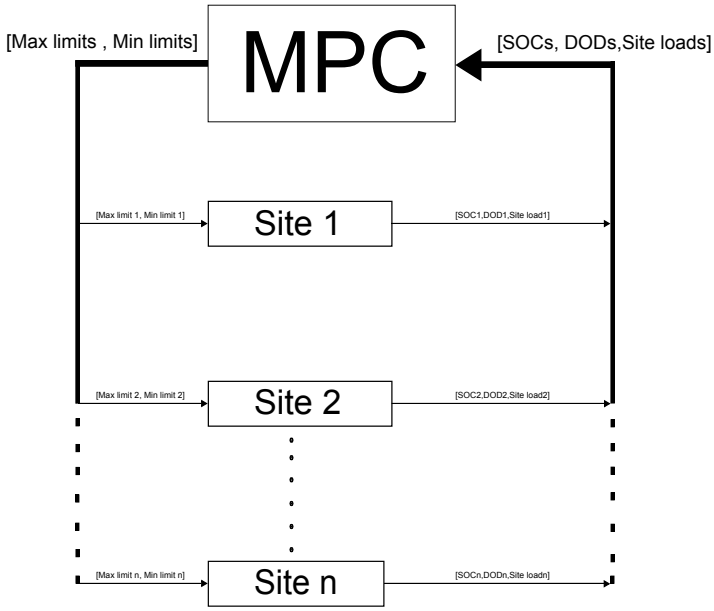

Figure 3.2: Overall system

3.2 Telecommunication Site

The MPC developed in this thesis is designed to control a certain number of communication-sites. Each of these sites consists of a battery, a rectifier and a some kind of communication equipment. The rectifier is used to convert the AC current in the grid to DC current that drives the communication load and charges the battery. Most sites may also have an inverter which allows the site to generate power back to the grid. Each site also has a controller which controls the power through the rectifier/inverter directly. There are two types of sites implemented in these simulations. One that has a BESS with lead-acid batteries, and one type which have a BESS made up of lithium-ion batteries. Both are inspired by the SIMULINK model suggested for PFR in (Energinet.dk, 2013). The site controllers are the same both for sites with lead-acid batteries and lihtium-ion batteries.

The battery models implemented in the sites are for one battery cell only, and the lithium-ion batteries that the lithium-ion degradation model is based on have cells that has a capacity of about $2Ah$. The lead-acid battery model uses cells of $54Ah$. Hence, the input to the models that calculates the degradation and SOC needs to be scaled down. It is assumed that the total amount of current into one BESS is distributed equally over each battery cell. This leads to that if a BESS made up of 600 cells and is charged with $1kW$, then the charging power of one cell is $1kW$ divided by the number of battery cells making up the BESS, which in this case becomes $1/600kW$. For a lead-acid BESS the charge power is divided by both the number of cells and the BESS voltage, which in these simulations are $48V$. This is to get the charge current, since in the lead-acid battery degradation model, the SOC is calculated by the charged/discharged Ah divided by the battery capacity in Ah. In the following equation, P_{cell} is the charge/discharge power for one cell, P_{BESS} is the total battery charge/discharge power, $C_{\text{cell,kWh}}$ is the cell capacity in kWh, while C_{BESS} is the BESS total capacity. Icell is the cell current, while I_{BESS} is the BESS current. $C_{\text{cell,Ah}}$ is the battery cell capacity in Ah, and $C_{\text{BESS,Ah}}$ is the BESS capacity in Ah.

$$P_{cell} = \frac{P_{BESS} C_{cell,kWh}}{C_{BESS,kWh}} \qquad I_{cell} = \frac{I_{BESS} C_{cell,Ah}}{C_{BESS,Ah}} \tag{3.1}$$

3.2.1 Lead Acid Battery Model

The battery model in the sites with lead-acid batteries useseqs. (2.7) and (2.12) to (2.20) to calculates the capacity loss, SOC and DOD with the current as input to the model. The DOD is calculated with the same equations as in 2.7, except that the battery current is used instead of the battery power throughput, and the capacity is in ampere-seconds in stead of watt-seconds. The Simulink model can be found in fig. 3.3, and the code for the MATLAB-function blocks are in appendix A.3. Some of the equations contains singularities. However, since the weighted number of cycles Z_W is calculated by integrating the discharged Ah by the capacity C_{battery}, the model only needs to work for negative currents I_{cell}. This means that where there are singularities, the output from these equations are ignored when I_{cell} are close to zero. For example, in eq. (2.18), f_I are set to be zero when the current is larger than $I_{\text{cell}} = -0.00005$. In the implementation of eq. (2.17), it is set to be zero if $|I_{\text{cell}}| < 0.00005$.

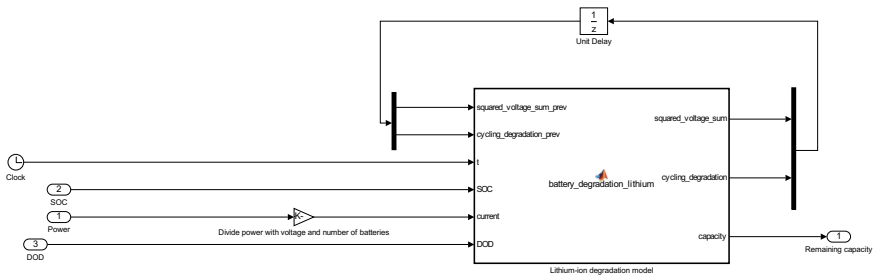

Figure 3.4: The simulation set-up for the lithium-ion batteries

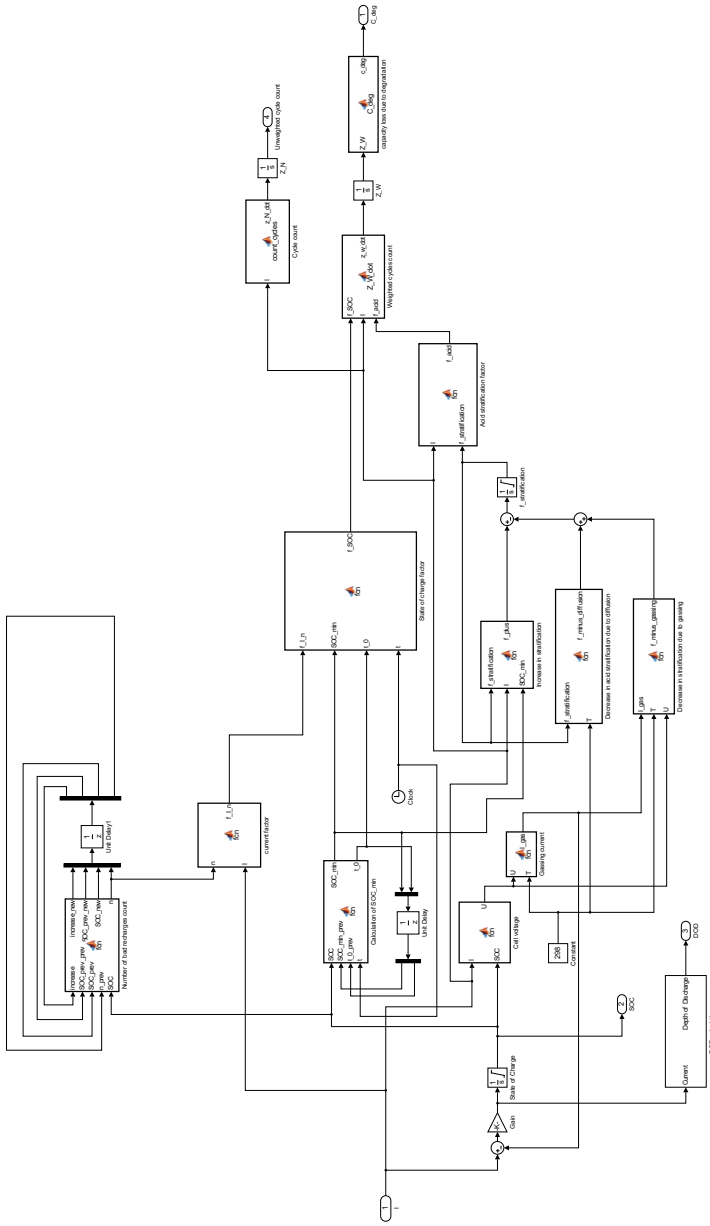

Figure 3.3: The simulation set-up for the lead-acid degradation model

3.2.2 Lithium-Ion Battery Model

The lithium-ion battery model uses the scheme from (Energinet.dk, 2013) to calculate the SOC with only the battery charge power as input. The DOD is calculated with the equations in 2.7 and the capacity loss is found from the model in eqs. (2.8) and (2.11). The degradation model is implemented as in fig. 3.4. Most of the calculation is done in the MATLAB-function which can be found in appendix A.4.1. It first uses the battery state of charge to calculate the cell voltage by using eq. (2.9). Then, the root mean square voltage is calculated by summing up all the squares of the voltages from the simulation starts and taking the square root of the mean of this sum. After this, the parameters β_{cap} and α_{cap} are calculated by eqs. (2.10) and (2.11). For the voltage in eq. (2.11), the voltage of time t is used. The variable Q is calculated by dividing the absolute value of the current with $3600s$ in order to get the units to be As instead of Ah.

3.2.3 Site controller

The site controller is equal both for a lead-acid site and a lithium-ion site and it consists of two branches. One is a P-controller which tries to maintain the battery level at a nominal level in order to reduce stress on the battery. This nominal level should be 100% for lead acid batteries since lead acid batteries prefer to be fully charged. For lithium-ion batteries however, the preferred battery level is about half-charged (Schmalstieg et al., 2014). In this scheme, this is not possible since the batteries are also used as backup power for critical communication equipment and therefore it is assumed that only the top 50% of the energy is available for PFC. This means that the nominal battery level should be as low as possible but high enough such that the actual battery level never breaches a lower bound of 50%. It is therefore set to 70%. The control gain for a site i, $K_{charge}(i)$, is calculated to be

$$K_{charge}(i) = \frac{1}{KC_{\text{BESS}}(i)} \tag{3.2}$$

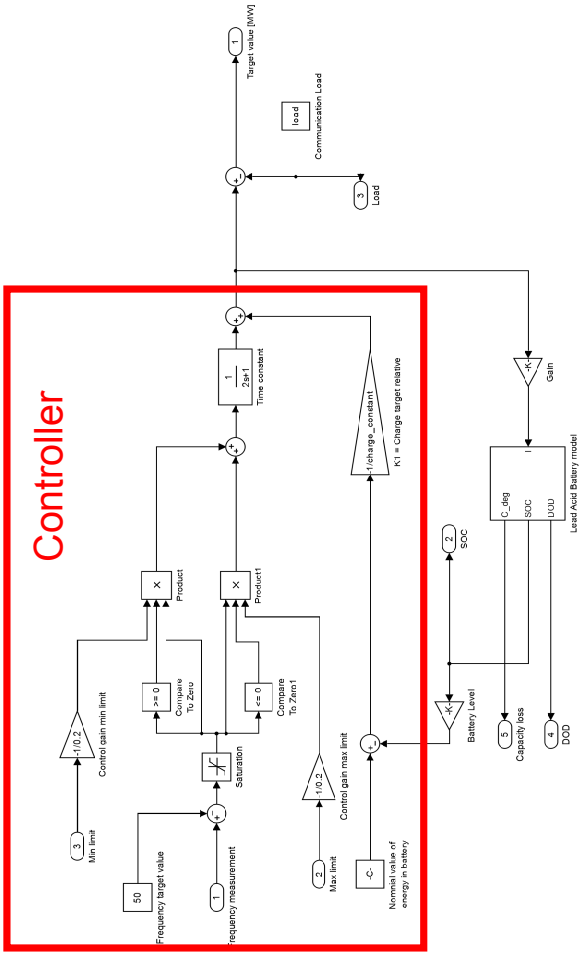

Figure 3.5: The site controller which controls the power throughput on each site for a lead acid site

This means that the amount of power that should be subtracted to or added to the power through the rectifier/inverter becomes

$$\begin{aligned} P_{\text{SOC compensation}}(i) &= -(\text{battery level}_{\text{ref}}(i) - \text{battery level}(i) K_{\text{charge}}(i) \\ &= -C_{\text{BESS}}(i) \frac{\text{SOC}_{\text{ref}}(i) - \text{SOC}(i)}{KC_{\text{BESS}}(i)} \\ &= -\frac{\text{SOC}_{\text{ref}}(i) - \text{SOC}(i)}{K} \end{aligned} \tag{3.3}$$

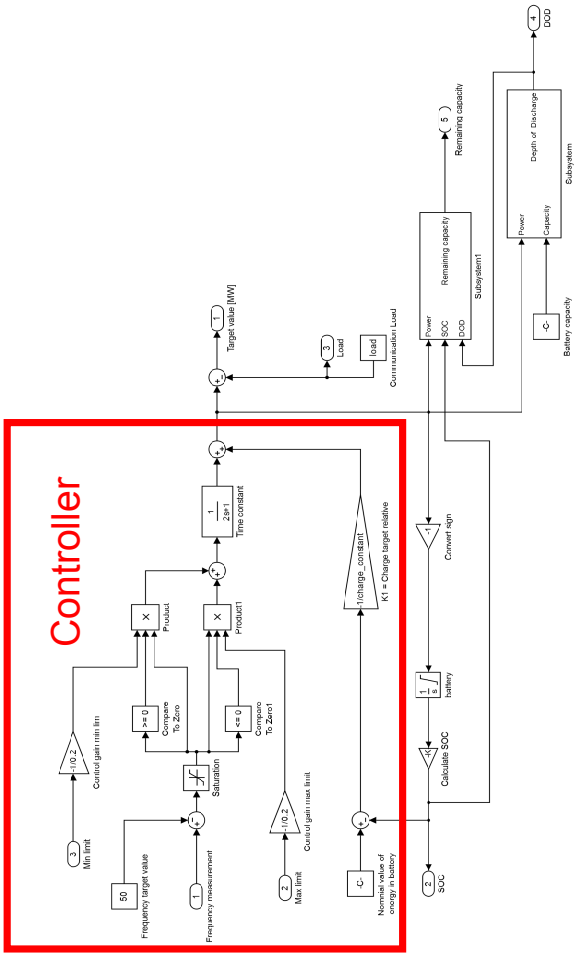

Figure 3.6: The site controller which controls the power throughput on each site for a lithium ion site

As seen from eq. (3.3), $P_{\mathrm{SOC}_{\mathrm{compensation}}}$ is independent of the BESS energy capacity. This means that both for a small and a big battery, the compensation power is equal for an equal deviation in the SOC. This also makes it difficult to test a distributed BESS against a single BESS, since every battery will get the same compensation power, the distributed energy storage will in total compensate with a significantly larger power than the single BESS given a specific deviation in the SOC from $\mathrm{SOC}_{\mathrm{ref}}$.

The other part of the controller can be seen on as a disturbance for the P-controller. It is the part of the site controller which decides how much power should be used for PFC(P_{PFC}). The inputs to this controller are maximum and minimum limits for the

power available for PFC (the charge/discharge power for the battery) and a frequency.

The frequency target value of $50Hz$ is subtracted from the frequency measurement to achieve the Δf. The Δf then goes through a saturation block , such that it will not be larger than $0.2Hz$. The minimum limit is taken in and multiplied with a gain according to the equations in 2.2, and then taken to a product block which multiplies the signal with a boolean which is equal to one when Δf is positive, and Δf. The maximum limit takes a similar route, but the boolean multiplied with the signals are 1 when Δf is negative. Since only one of these two branches can be non-zero, they are added together and delayed two seconds before the signal is added together with the signal from the P-controller and sent to the rectifier/inverter. Before the signal is given to the inverter/rectifier, the communication power is subtracted. The communication load is not subtracted from the rectifier/inverter throughput before after the power is given to the battery. This is done because the load power is not considered to discharge the battery as long as the load may get its power from the grid.

3.3 Economics

PFC is a profitable service (Thorbergsson et al., 2013). How profitable it is, depends on, among other factors, how many bids are won. In the simulations conducted in this thesis, it is assumed that all bids are won. In Germany, the revenues from PFC have in the past lay between 2000€/MW/week and 4000€/MW/week. The profit for one week is in this thesis calculated to be the income from PFC minus the cost of battery degradation. The cost of battery cycling D_{cost} is calculated as the number of times the battery is cycled times the battery price divided by the maximum cycle count before the battery must be replaced. In the following equation, N is the number of times the battery is cycled, ρ is the battery price per kWh, C_{battery} is the battery capacity and $N_{\text{EOL,cycles}}$ is the number of times a battery can be cycled before it reaches its end of life.

$$D_{cost} = \frac{N_{\text{cycles}} \rho C_{\text{BESS}}}{Z_{\text{IEC}}} \tag{3.4}$$

Type of Variable	Variable Name	Description
CV	$x_{\text{SOC,max}}$	SOC in all BESSs at $\Delta f = -0.2$ for k = 1,...,L, given $u_{\max}$
CV	$x_{\text{SOC,min}}$	SOC in all BESSs at $\Delta f = 0.2$ for k = 1,...,L given $u_{\min}$
CV	$x_{\text{DOD,max}}$	DOD in all BESSs at $\Delta f = -0.2$ for k = 1,...,L, given $u_{\max}$
CV	$x_{\text{DOD,min}}$	DOD in all BESSs at $\Delta f = 0.2$ for k = 1,...,L given $u_{\min}$
DV	Z	Binary vector with length N. If site i is available for PFC, $Z(i) = 1$
DV	Δf	Frequency deviation
DV	P_{load}	Site load power
MV	$u_{\max}(i)$	Maximum Δf up-regulation for site i
MV	$u_{\min}(i)$	Maximum Δf down-regulation for site i

Table 3.1: An overview of the variables for MPC1 and MPC2

3.3.1 MPC controller 1

This is the MPC controller used for reference. It is inspired by the control strategy in (Teleke et al., 2010) where the goal is to minimize the deviation between the power output and a power reference which tells the controller how much power that shall be drawn from the battery energy storage system (BESS). The objective function differs from the one in the model of a typical MPC in 2.22, but it is still a quadratic function, hence it is still a convex optimization problem.

$$J = (Z^T u_{max} - P_{ref,up})^2 + (Z^T u_{min} - Z^T P_{\text{load}} - P_{ref,down})^2 \tag{3.5a}$$

s.t. (3.5b)

$$x_{SOC,max}(k+1,i) = x_{SOC,max}(k,i)(1 - \frac{1}{K_{charge}}) + \frac{SOC_{ref}}{K_{charge}} - \frac{u_{max}(i)}{C_{battery}}, k = 1,...,L, i = 1,...,N \tag{3.5c}$$

$$x_{SOC,min}(k+1,i) = x_{SOC,min}(k,i)(1 - \frac{1}{K_{charge}}) + \frac{SOC_{ref}}{K_{charge}} + \frac{u_{min}(i)}{C_{battery}}, k = 1,...,L, i = 1,...,N \tag{3.5d}$$

$$SOC_{min} \leq x_{SOC,max}(k,i) \leq SOC_{max}, k = 1,...,L, i = 1,...,N \tag{3.5e}$$

$$SOC_{min} \leq x_{SOC,min}(k,i) \leq SOC_{max}, k = 1,...,L, i = 1,...,N \tag{3.5f}$$

$$0 \leq u_{max}(i) \leq I_{cap}(i) - P_{\text{load}}(i), i = 1,...,N \tag{3.5g}$$

$$0 \leq u_{min}(i) + P_{\text{load}}(i) \leq R_{cap}, i = 1,...,N \tag{3.5h}$$

$I_{\text{cap}}(i)$ is the inverter capacity of site i, and $R_{\text{cap}}(i)$ is the rectifier capacity at site i. This controller minimizes the difference between the sum of $u_{\max}$ and $P_{\text{ref,up}}$. The part of the

objective function for $u_{\min}$ also includes the site load P_{load} since the site loads occupy some of the rectifier capacity. However, the site load makes the capacity for Δf up-regulation larger. It also states that $x_{SOC,max}(k,i)$ and $x_{SOC,min}(k,i)$ should be kept between the limits SOC_{max} and SOC_{min}.

3.3.2 MPC controller 2

This is the main MPC controller developed in this paper. It is basically a distributed version of the controller developed in (Koller et al., 2013). The main goal of this controller is to deliver the set amount of power and at the same time minimizing the square of the depth of discharge. The intention of this is that the power will be distributed in such a way that the cycle depth is equal in every battery pack.

$$J = \sum_{k=1}^{L}\sum_{i=1}^{N} x_{DOD,max}(i,k)^T Q_{max} x_{DOD,max}(i,k) +$$
$$\sum_{k=1}^{L}\sum_{i=1}^{N} x_{DOD,min}(i,k)^T Q_{min} x_{DOD,min}(i,k) +$$
$$S_1 P_{\text{slack,up}} + S_2 P_{\text{slack,down}} \tag{3.6a}$$

s.t.

$$x_{SOC,max}(k+1,i) = x_{SOC,max}(k,i)(1-\frac{1}{K_{charge}}) + \frac{SOC_{ref}}{K_{charge}} - \frac{u_{max}(i)}{C_{battery}} \tag{3.6b}$$

$$x_{SOC,min}(k+1,i) = x_{SOC,min}(k,i)(1-\frac{1}{K_{charge}}) + \frac{SOC_{ref}}{K_{charge}} + \frac{u_{min}(i)}{C_{battery}} \tag{3.6c}$$

$$x_{DOD,max}(k+1,i) = A_d x_{DOD,max}(k,i) +$$
$$B_d(\frac{x_{SOC,max}(k,i) - SOC_{ref}(i)}{K_{charge}} + \frac{u_{max}(i)}{C_{battery}}) \tag{3.6d}$$

$$x_{DOD,min}(k+1,i) = A_c x_{DOD,min}(k,i) +$$
$$B_c(\frac{SOC_{ref}(i) - x_{SOC,min}(k,i)}{K_{charge}} + \frac{u_{min}(i)}{C_{battery}}) \tag{3.6e}$$

$$Z^T u_{max}(i) = P_{ref,up} - P_{slack,up} \tag{3.6f}$$

$$Z^T u_{min}(i) = P_{ref,down} - P_{slack,down} \tag{3.6g}$$

$$SOC_{min} \leq x_{SOC,max}(k,i) \leq SOC_{max} \tag{3.6h}$$

$$SOC_{min} \leq x_{SOC,min}(k,i) \leq SOC_{max} \tag{3.6i}$$

$$0 \leq u_{max}(i) \leq I_{cap} - P_{\text{load}}(i) \tag{3.6j}$$

$$0 \leq u_{min}(i) + P_{\text{load}}(i) \leq R_{cap} \tag{3.6k}$$

$$0 \leq P_{slack,up} \leq P_{ref,up} \tag{3.6l}$$

$$0 \leq P_{slack,down} \leq P_{ref,down} \tag{3.6m}$$

The manipulated variables (MVs) of this MPC is a vector of two limits for each site. The limits are thought to be constant over the prediction horizon. The upper limit $u_{\max}$ tells a designated site how much power it can deliver to the grid, while the lower limit $u_{\min}$ tells the site how much power it can pull from the grid. The power limits $u_{\max}$ and $u_{\min}$ are calculated to be the limits that gives the optimal distribution of power for the frequency where maximum power output is required ($|\Delta f| = 0.2Hz$). The u_{max} is the set of limits that minimizes the sum of the square of the DOD in each battery considering that the state of charge $x_{SOC,max}(k,i)$ and $x_{SOC,min}(k,i)$ should not go below a certain limit on each site. u_{min} minimizes the sum of the squared DODs when charging the battery. The first double sum in the objective function J represents the DOD for discharging, while the second represents the DOD for charging. It is also important to note that as the limits of the droop curve changes, the slope of the curve also changes. The controlled variables (CVs) are then the SOC ($x_{SOC,min}(k,i)$, $x_{SOC,max}(k,i)$) and DOD ($x_{DOD,max}(k,i)$ and $x_{DOD,max}(k,i)$) on each site. The disturbance variables (DVs) are the frequency Δf and the load Pload on each site. Here, the frequency is a non-measured DV since it is not used in the MPCs calculations, even though it is measured and used on site level. The load is a measured disturbance, and is sampled at the start of each iteration in the MPC and assumed to be constant throughout the prediction horizon. The assumption is then that the load power is slowly or not varying at all, or the prediction horizon is short enough to make this assumption valid. The Z vector is a binary vector where $Z(i)$ is equal to 1 when site number i is available for primary frequency control. $P_{slack,up}$ and $P_{slack,down}$ are slack variables for the power constraints. The weights on these are S_1 and S_2.

The $x_{DOD,max}$ variable is the cycle depth caused by discharging the batteries at the maximum frequency deviation, and $x_{DOD,min}$ is the cycle depth caused by charging the batteries at the maximum frequency. The objective of this MPC is then to make these cycle depths as evenly distributed as possible. $x_{SOC,max}$ and $x_{SOC,min}$ is the state of charge and is calculated in the prediction by assuming maximum negative frequency deviation $x_{SOC,max}$ and for $x_{SOC,min}$, maximum positive frequency deviation is assumed. The idea is that since this is the worst case scenario, the limits the MPC calculates makes sure that none of the sites breaches its SOC limits.

Chapter 4

Results

This chapter consists mainly of three parts. Sections 4.1 to 4.5 describes the functionality of the MPC controllers, while section 4.6.1 deals with tuning of the weight matrices of the objective function of the controller, and at last, some degradation tests in **????**. The functionality tests are, unless something else is stated, run with MPC2. The results of these tests for MPC1 are identical. All tests uses the same simulation set-up with 20 sites, where 10 sites have lead-acid batteries, and 10 sites have lithium-ion batteries. It is assumed that each site have one battery-pack, and this can be seen as one battery. The voltage over each battery is $48V$. The capacities are distributed as in tables 4.1 and 4.2. The simulation sample-time is 1 second, while the MPC is set to have a sample-time of 10 seconds.

4.1 Acceptance test

These simulations are run in order to explain how the MPCs works, and show that they follow the demands of the Danish TSO Energinet.dk. The test lasts for 5 hours, and the plant must deal with three different obstacles in order to pass the test. The first of

Lead-acid batteries

Site number	1	2	3	4	5	6	7	8	9	10
$\mathbf{C_{battery}}$**(kWs)**	207360	224640	172800	207360	190080	155520	241920	259200	224640	190080
$\mathbf{C_{battery}}$**(Ah)**	1200	1300	1000	1200	1100	900	1400	1500	1300	1100

Table 4.1: Table of battery capacities at each lead-acid site.

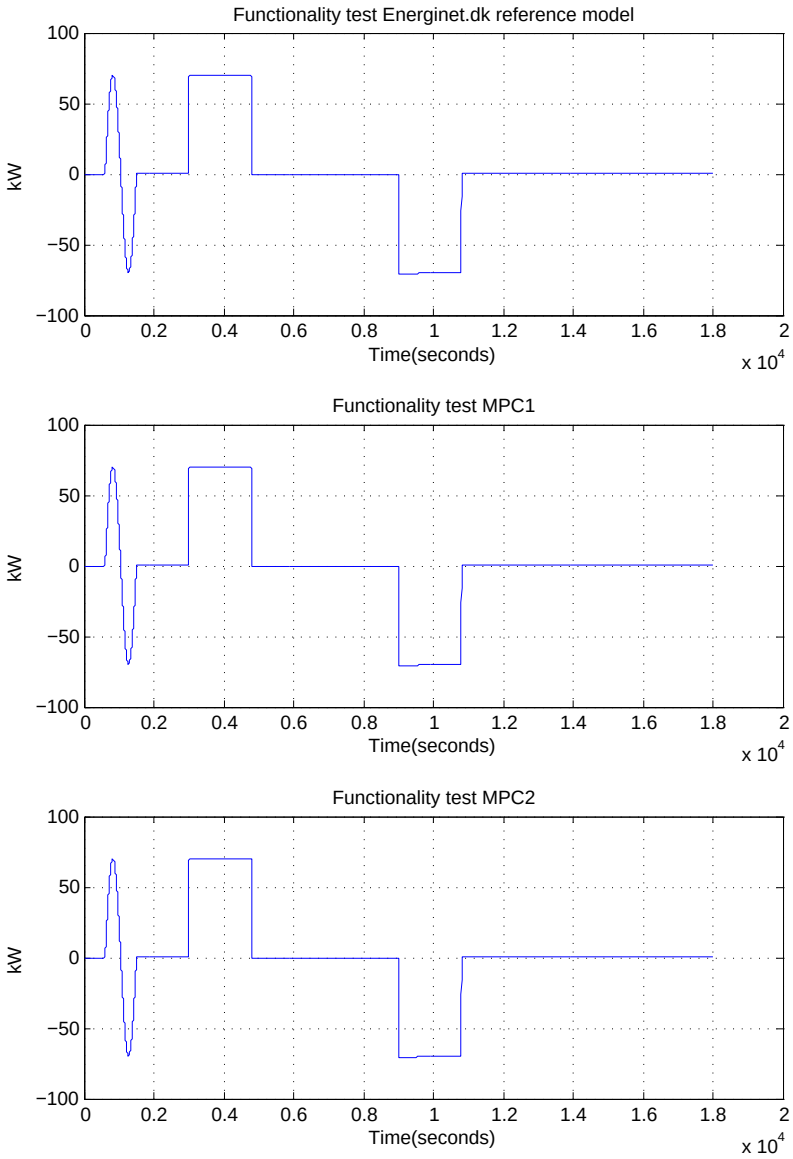

Figure 4.1: A simulation performed with one site which delivers symmetrical 70kW and a BESS of

Lithium-ion batteries

Site number	11	12	13	14	15	16	17	18	19	20
$\mathbf{C_{battery}}$**(kWs)**	207360	224640	172800	207360	190080	155520	241920	259200	224640	190080
$\mathbf{C_{battery}}$**(Ah)**	1200	1300	1000	1200	1100	900	1400	1500	1300	1100

Table 4.2: Table of battery capacities at each lithium-ion site.

these obstacles is a frequency deviation that follows a sine wave with an amplitude of $0.2Hz$. This is in order to verify that the plant can react fast enough. After the plant has rested for a period, it needs to endure one period of maximum negative frequency deviation and one period of maximum positive frequency deviation, each of 30 minutes. In the first time period $\Delta f = -0.2$ and in the second, $\Delta f = 0.2$. This is to verify that the total plant battery capacity are large enough to participate in PFC. In the first plot in fig. 4.2, a reference test is run where the plant consists of only one site with a battery-pack of $4147200kWs$. This site is supposed to deliver a symmetrical 70kW at maximum frequency deviation in both directions. In the two other plots in fig. 4.2, two test runs with a distributed system with 20 sites with a total amount of $4147200kWs$ dsitributed among the battery-packs as in tables 4.1 and 4.2, and each site is equipped with a rectifier and an inverter where all rectifiers have a capacity of 8kW, and the inverters also have a capacity of 8kW each. This enables all the sites to deliver 8kW in both directions. The plant is made up of 20 different sites, which implies that the maximum power output from the overall plant, both for Δf up-regulation and Δf down-regulation, is 160kW. However, in this simulation, the MPC is told that the plant only should deliver a symmetrical 70kW at maximum frequency deviation. The paramaeter K, which decides the control gain in the SOC compensation controller-part of the site-controllers, is in these simulations set to be equal to 1, which gives such a small compensation value that it can be neglected. This is done because of the implications of equation 3.3. In the tests in fig. 4.3 , $K = 0.004$ to enable SOC compensation in order to spare the batteries. This is similar to the tests done by Energinet.dk (Energinet.dk, 2013).

4.2 Dynamic number of sites

This test was carried out to verify that the controllers can handle the situation that occurs when one ore more sites for some reason suddenly cannot deliver power for PFC.

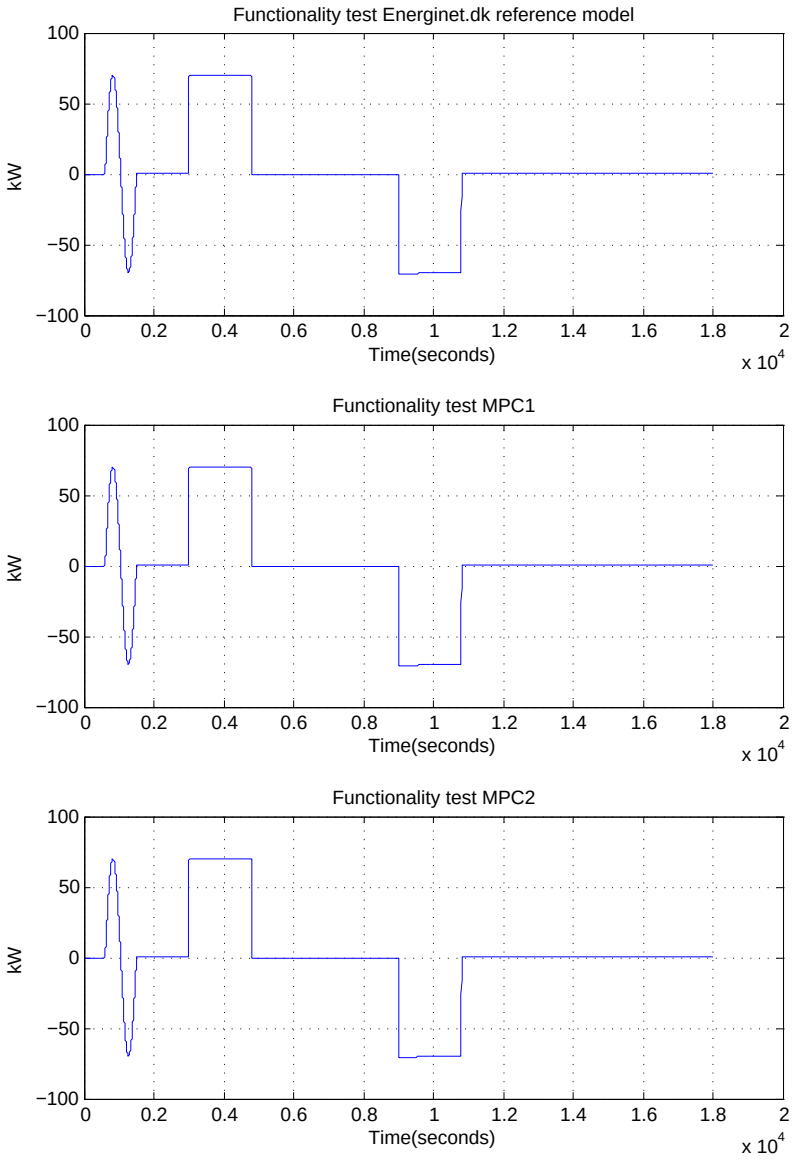

Figure 4.2: A simulation performed with one site which delivers symmetrical 70kW and a BESS of

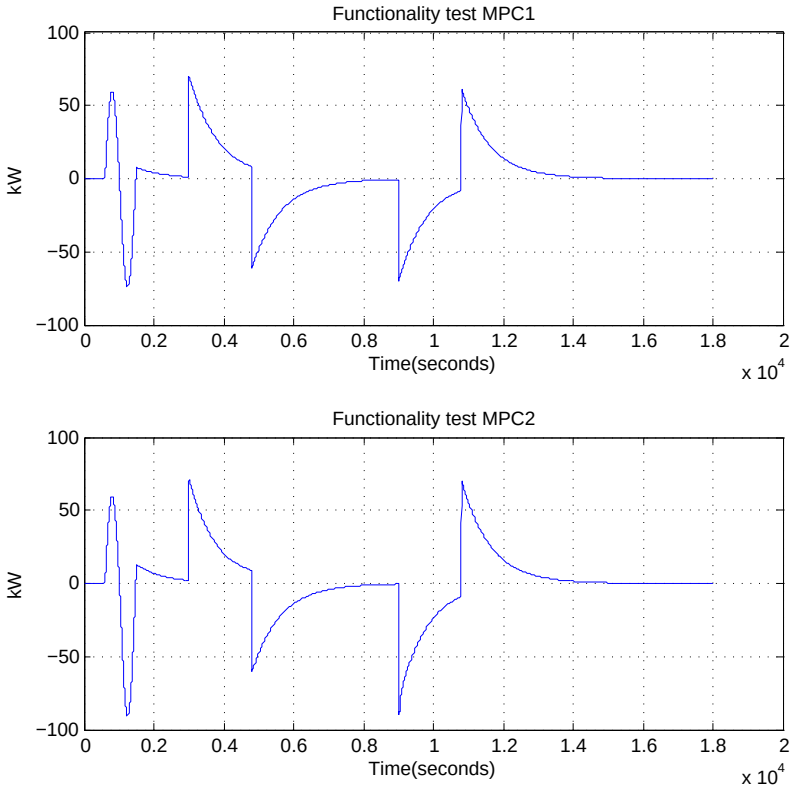

Figure 4.3: Simulations performed with MPC1 and MPC2 with SOC compensation.

The test is carried out with the same set-up as the acceptance tests in fig. 4.3. During this test, there are two sites that are taken out. One site with a lithium-ion battery which stops delivering power from $t = 5000s$ to $t = 10000$, and one site with a lead-acid battery which is taken out between $t = 600s$ to $t = 4000s$. The plots that can be found in fig. 4.4, shows the limits both for up-regulation and down-regulation for the two batteries that are disabled for PFC. Those plots shows that the limits are set to zero by the MPC at the correct time. The down regulation limit for the lead-acid battery is also zero after about $t = 9000s$. However, the reason for this is that the battery is fully charged. The third plot shows the total amount of power made available for PFC by the MPC. As can be seen by the third plot in fig. 4.4, this is always 70kW for both up- and down-regulation in this

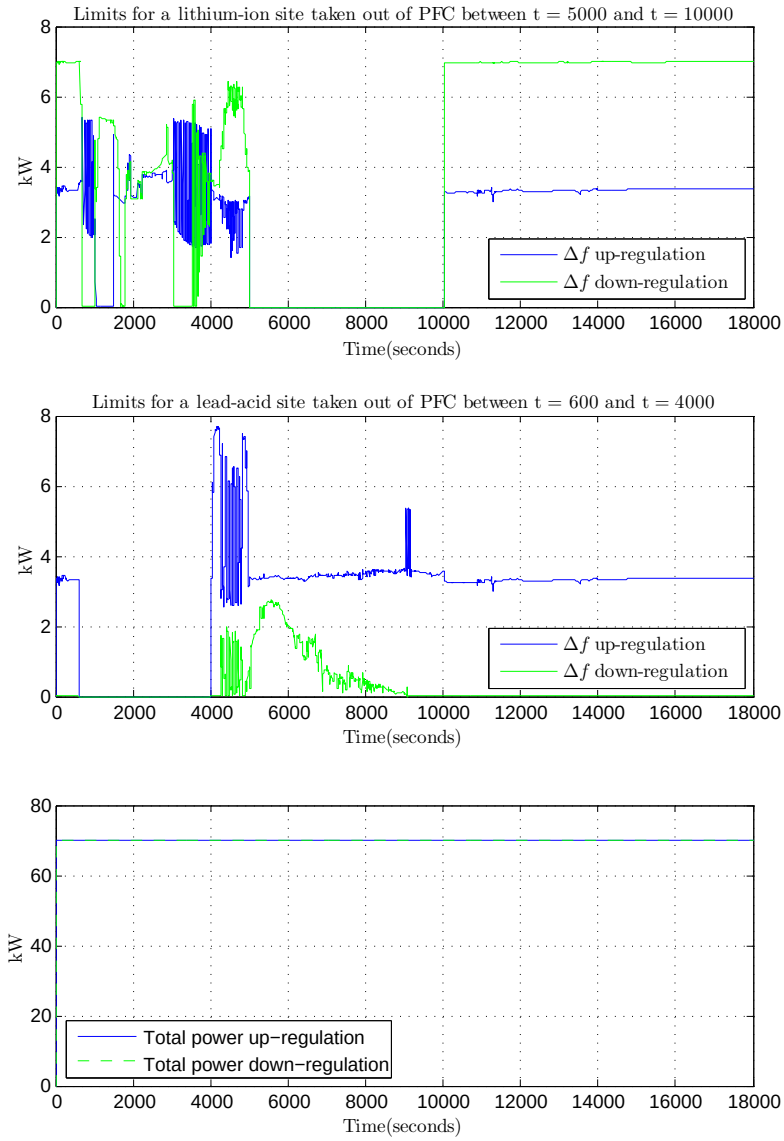

Figure 4.4: Simulation where two sites are not able to use for PFC at different time intervals.

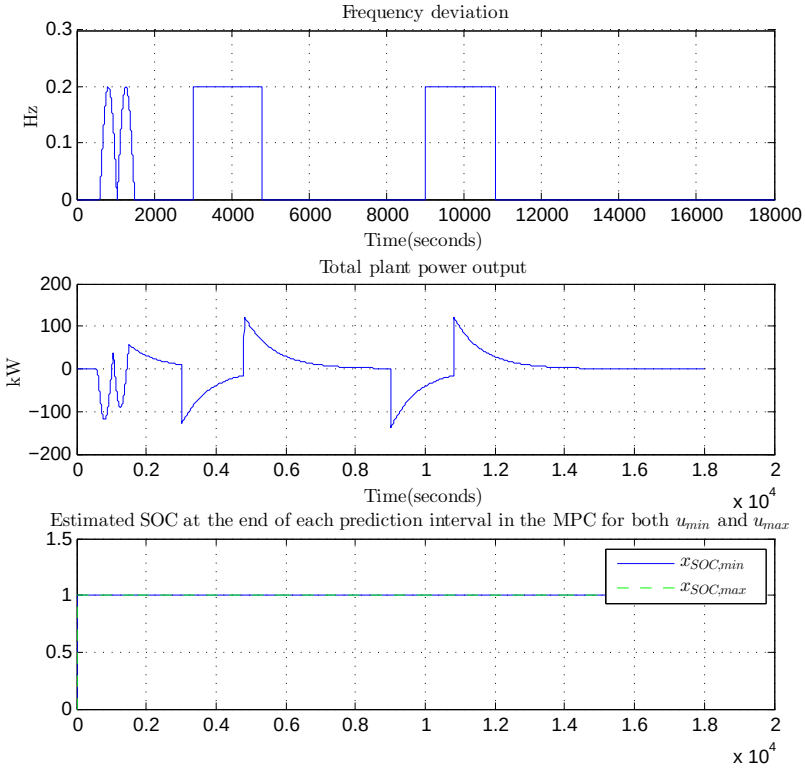

Figure 4.5: Test scheme for testing the constraints of the MPC

simulation, meaning that the two sites taken out does not affect the plants ability to deliver PFC according to the TSOs regulations. The total power output is not included here, since it is identical to the power outputs in fig. 4.3.

4.3 MPC constraint test

In order to test whether the MPC can keep plant inside its constraints, which are the maximum and minimum limits for the SOC, the saturated integrators used in the site controller was replaced with unsaturated ones. Slack variables was added to the MPC-controller such that it was still able to find a solution even if the battery level in one

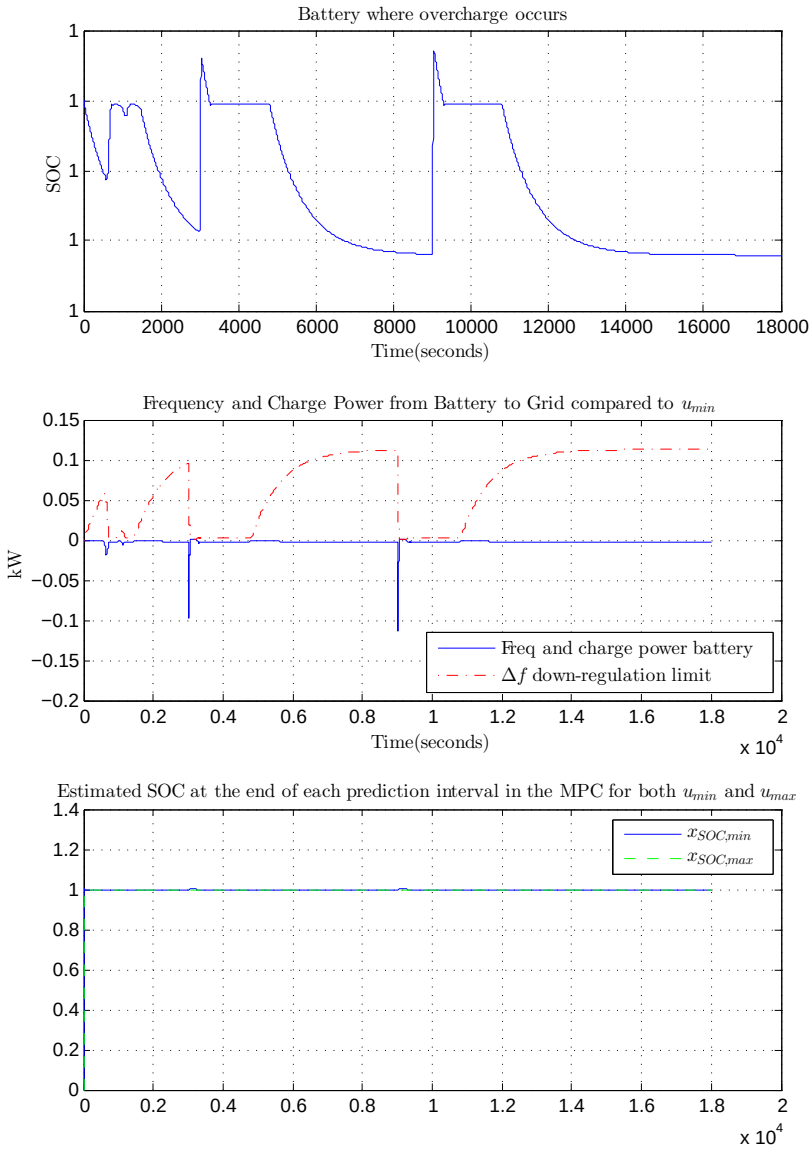

Figure 4.6: Testing if the MPC is able to keep the battery levels inside the constraints set.

of the sites went out of bounds. This is what happens in the tests in figs. 4.5 and 4.6. The test that is run is similar to the one in fig. 4.3, with one difference, namely that the frequency deviations are always positive, meaning that the plant should only down-regulate the frequency, which means charging the batteries. The frequency deviation and the total plant power-output are shown in fig. 4.5. The first plot shows the SOC in one lead-acid battery, and what it shows is that at first, the battery level is sinking due to the I_{gas} current. This then makes the battery level low enough such that the MPC allows the battery to participate in PFC, which can be seen by the Δf down regulation limit rising in the second plot in fig. 4.6. When a frequency deviation occurs, the battery level rises slightly higher than 1. This is not because of the SOC compensation controller at each site, since this controller gives zero power when SOC is equal to SOC_{ref}. The third plot in fig. 4.6 shows the SOC values for a lead-acid battery at the end of the prediction horizon of the MPC. As the plot shows, at the peaks of the actual battery levels, the solutions of the MPC is slightly more than 1 becuase of the slack variables. The third plot in fig. 4.5 is the SOC for a lead-acid battery at the end of the prediction horizon run in a similar test, but with saturated integrators. As can be seen from this plot, the SOC level calculated in the MPC is never higher than 1. This shows that as long as the MPC is given a start point smaller than or equal to 1, its solutions should never allow a site to charge its battery over fully charged.

4.4 Slack variables test

This simulation was run in order to show how the slack variables for the power works. It was run with the same set-up as the reference test, but between $t = 8000s$ to $t = 10000s$, seven of the ten lithium-ion sites were set to not contribute to PFC. As seen from the plot of the total frequency and charge power from batteries to the grid in fig. 4.7, between $t = 8000s$ to $t = 10000s$, the system cannot deliver the amount of power it is supposed to. However, the MPC still finds a solution due to the slack variables. The second plot shows the limits given from the MPC to a specific lithium-ion site, and it is seen that between $t = 8000s$ and $t = 10000s$ both limits are zero. In this time period, ten lead-acid batteries and three lithium-ion batteries can contribute to PFC. The capacities of the rectifiers and inverters are set to $8kW$, which means that $104kW$ is a available for

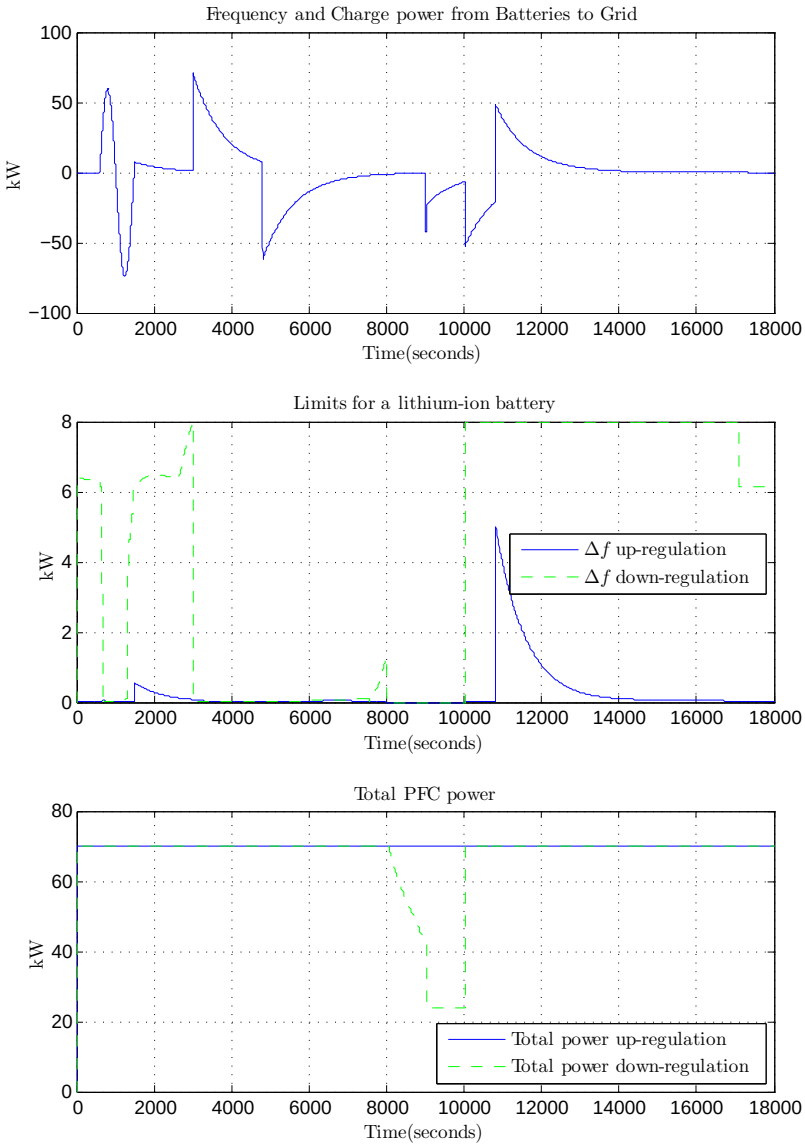

Figure 4.7: Simulation run with MPC2 where a large number of sites cannot participate in PFC

PFC. However, when the lead-acid batteries fills up, they cannot contribute to Δf down-regulation since this means over-charging the batteries. From the third plot in fig. 4.7 it is shown that the total amount of power available for down-regulation is gradually sinking as the lead-acid batteries fills up until it hits the bottom at $24kW$, which is the capacity of the three lithium-ion batteries still available for PFC.

4.5 Testing how much power the plant may deliver

This simulation is run in order to clarify how much power the total plant can promise to deliver. The total rectifier capacity is $160kW$, but seven of the lead-acid sites are missing inverters, making the total inverter capacity $104kW$. The total power output from the plant at maximum frequency deviation is set to be $170kW$ which is, obviously, more than the plant can handle. Each site should also serve a load of $1kW$. The Δf up-regulation capacity is then the inverter capacity plus the site load, which is $124kW$ which is verified by the plots of the total frequency and charge power plot and the plot of the sums of the limits for up/down regulation in fig. 4.8. The total power output available for down-regulation is the sum of the rectifier capacities on the lithium-ion sites, which is $80kW$ plus the capacities of the lead acid batteries that are not fully charged minus the loads on all of the sites. This is verified by the plot of the sum of the site limits and the plot of the battery level for a lead-acid battery in fig. 4.8. Where the limits for Δf down regulation is rising when the battery level in the lead-acid battery is sinking.

In fig. 4.9, the limits for a single lead-acid site is shown. There is no inverter on the site, but the Δf up-regulation is still equal to $1kW$ because of the site load of $1kW$. The power output for frequency regulation without the charge power from the SOC-compensation is shown in the second plot in fig. 4.9, and the third plot shows that after adding the charge power from the SOC-compensation and the site load. The power output from the site is always negative, even though it contributes to Δf up-regulation.

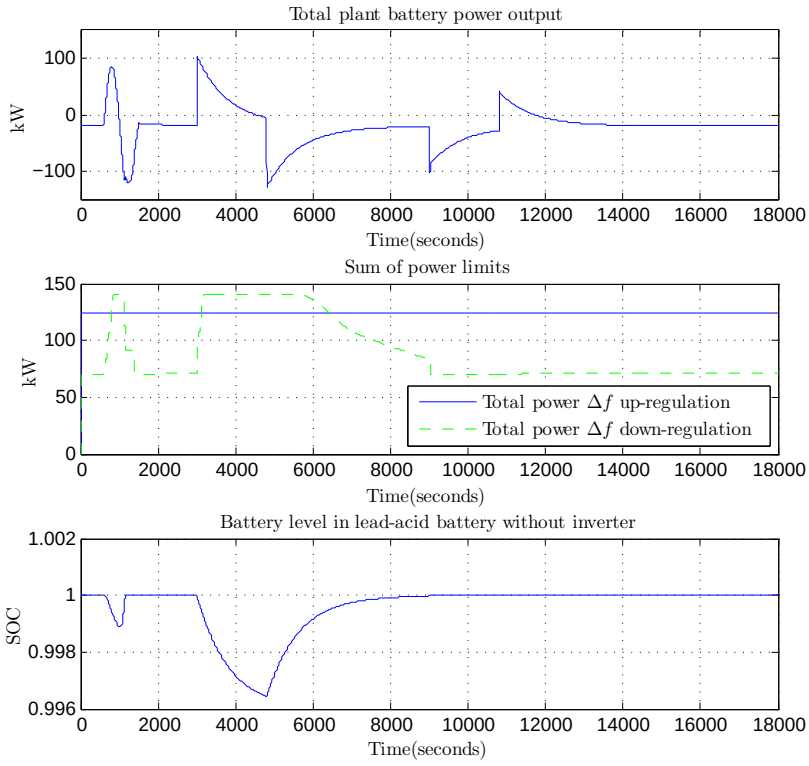

Figure 4.8: Simulation run where the requested power output is a symmetrical 170kW, which is more than both the rectifier and inverter capacity

4.6 Degradation simulations

All the degrdation results can be found in tables 4.6 and 4.7, since they all yield the same results as the test in fig. 4.10. The only difference is the degradation resuls, and it is the degradation at the end of the simulation that is interesting. Table 4.6 contains the average battery degradation calculated by the degradation models described in **????**. The column containging the results for the lead-acid batteries contains the average degradation results for the 10 lead-acid batteries, and the column with the results for the lithium-ion batteries contains the average degradation results for the 10 lithium-ion batteries. Table 4.7 contains the average cycling numbers for the

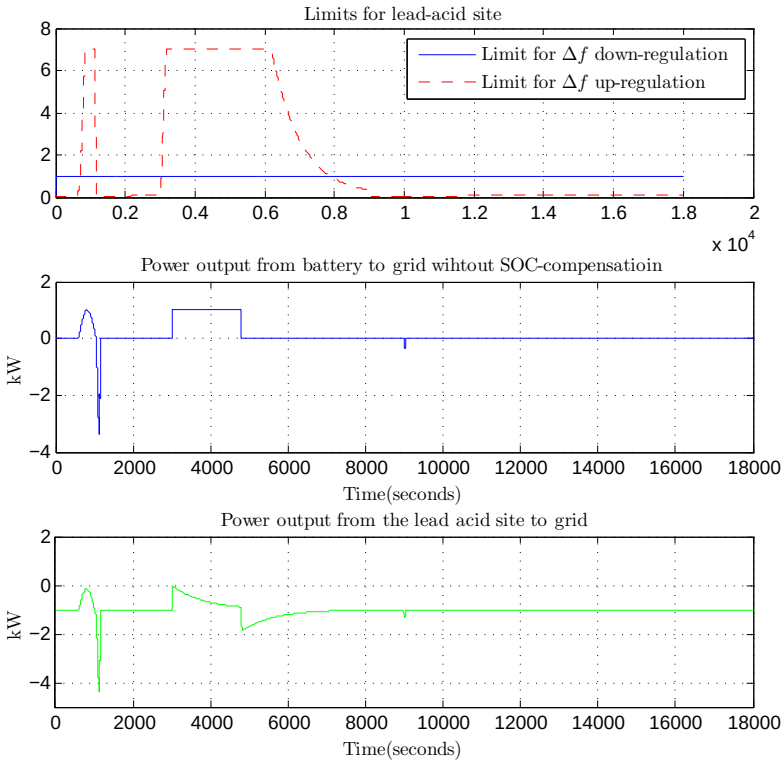

Figure 4.9: Simulation run where the requested power output is a symmetrical 170kW, which is more than both the rectifier and inverter capacity

4.6.1 Tuning of the MPC

The tuning tests are run with the same set-up as the reference test, except that it is run for 500000 seconds and the frequency deviation measurements are taken from a real data-set collected in Denmark August 2012. The goal of these simulation is to find the tuning of the Q-matrices in MPC2 which minimizes the battery cost. All Q-matrices used are diagonal matrices. The first test in tables 4.6 and 4.7 are run with equal weighting on all elements. Which means the diagonals in $Q_{\max}$ and $Q_{\min}$ consists of ones. The second test in tables 4.6 and 4.7 are run with no weighting at all on the lead-acid BESSs, which means that the elements of the diagonal of the Q-matrices corresponding to a

lead-acid BESS, is set to zero. In the simulations run here, that means that the ten first elements of the diagonal of $Q_{\max}$ and $Q_{\min}$ are set to 0, while the last ten elements on both diagonals are set to 1. In the third test in tables 4.6 and 4.7, there are no weight on down-regulation for lead-acid batteries. This done by leaving $Q_{\max}$ equal to the identity-matrix, and setting the first half of the diagonal of $Q_{\min}$ to 0. The fourth test in **??** and table 4.7, is run by not having any weights on the lithium-ion batteries. This is done by setting the diagonal of both $Q_{\max}$ and $Q_{\min}$ to have ones on the elements corresponding to the lithium-ion batteries. In these simulations these are the 10 last elements of each diagonal. As can be seen from this test, the lead-acid batteries are left unused. In test number 5 in tables 4.6 and 4.7, MPC1 is used instead of MPC2. This is done in order to test the performance of MPC2 versus the more naive approach used in the design of MPC1. In fig. 4.10 is an example of plots of the battery degradation, total power plots and frequency deviation plots. In appendix B, a simulation is run with more extensive plotting.

4.6.2 Cycle Depth Test

In order to verify that MPC2 optimizes the distribution of the power such that the sum of the squares of the DOD, two tests were run to compare it with MPC1. Bot tests run for 18000s, and the first test used the measurements of frequency deviation from Denmark taken in August 2012, but the second test was run with the same frequency deviations multiplied by ten. The Q-matrices of MPC2 in these tests weighed lead-acid and lithium-ion batteries equally as test 1 in tables 4.6 and 4.7. The results can be found in table 4.3

	MPC1	MPC2
RegularΔf	0.0216	0.0504
$10 \times \Delta f$	1.0733	3.6453

Table 4.3: Table that shows the sum of the squares of the DODs for all sites at each time-step.

4.6.3 Other Degradation Tests

In tests 6 and 7 in table 4.6, two tests are run which is performed similar to tests 1-5. However, new battery capacities, which are found in tables 4.4 and 4.5 ,are introduced

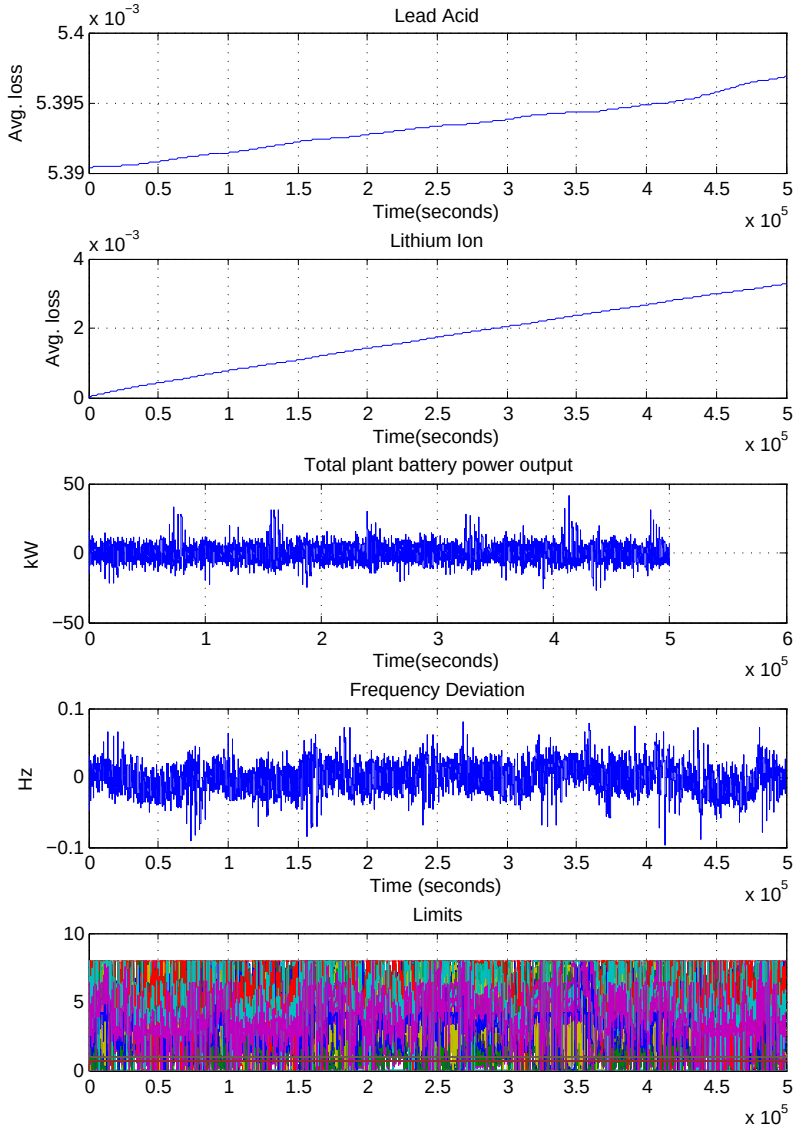

Figure 4.10: Degradation test performed with equal weighting on Q-matrices

Lead-acid batteries										
Site number	1	2	3	4	5	6	7	8	9	10
$\mathbf{C_{battery}}$**(kWs)**	86400	120690	155520	207360	241920	86400	120690	155520	207360	241920
$\mathbf{C_{battery}}$**(Ah)**	500	700	900	1200	1400	500	700	900	1200	1400

Table 4.4: Table of battery capacities at each lead-acid site

Lithium-ion batteries										
Site number	11	12	13	14	15	16	17	18	19	20
$\mathbf{C_{battery}}$**(kWs)**	86400	120690	155520	207360	241920	86400	120690	155520	207360	241920
$\mathbf{C_{battery}}$**(Ah)**	500	700	900	1200	1400	500	700	900	1200	1400

Table 4.5: Table of battery capacities at each lithium-ion site

to find out which controller handles this scenario better.

4.6.4 Economical results

In table 4.8, the economical results from the cycling tests are gathered. The tests are calculated by subtracting the cycling cost from both the lead-acid and lithium-ion batteries from the revenue in the 500000s period. The revenues depend on how much power that was made available in the period. For tests 1-7 in table 4.7, 70kW was made available, while in tests 8-10, 140kW was made available. This gives revenues of 115.5 and 231.5, respectively.

Test	**Description**	**Average Degradation**	
		Lead-acid	**Lithium-ion**
1	Equal weight on Lead-acid and Lithium-ion sites	6.6×10^{-6}	3.2716×10^{-3}
2	No weight on Lead-acid sites	1.84^{-5}	2.6869×10^{-3}
3	No weight on down-regulation for Lead-acid sites	7.2×10^{-6}	3.2272×10^{-3}
4	No weight on Lithium-ion sites	0	3.6111×10^{-3}
5	MPC1	7.2×10^{-6}	3.2419×10^{-3}
6	MPC1 higher variance in battery capacities	9.5×10^{-6}	3.5168×10^{-3}
7	MPC2 higher variance in battery capacities	2.37×10^{-5}	2.8731×10^{-3}
8	MPC2 with higher rectifier and inverter capacities	5.09×10^{-5}	3.3605×10^{-3}
9	MPC1 with higher rectifier and inverter capacities	1.74×10^{-5}	4.0321×10^{-3}
10	MPC2 high power capacity and no weighting on lithium-ion sites	0	4.5454×10^{-3}

Table 4.6: Average battery degradation at the end of simulation

Test	Description	Average number of cycles	
		Lead-acid	Lithium-ion
1	Equal weight on Lead-acid and Lithium-ion sites	0.1484	0.6324
2	No weight on Lead-acid sites	0.3176	0.4165
3	No weight on down-regulation for Lead-acid sites	0.1615	0.6086
4	No weight on Lithium-ion sites	7.16×10^{-3}	0.8519
5	MPC1	0.1579	0.637
6	MPC1 higher variance in battery capacities	0.1986	0.861
7	MPC2 higher variance in battery capacities	0.3972	0.5502
8	MPC2 with higher rectifier and inverter capacities	0.7094	0.8286
9	MPC1 with higher rectifier and inverter capacities	0.3115	1.1073
10	MPC2 high power capacity and no weighting on lithium-ion sites	6.7436×10^{-3}	1.3536

Table 4.7: Average number of cycles at the end of simulation

Economic Calculations										
Test	1	2	3	4	5	6	7	8	9	10
Cycle Cost Lead-acid	15.5€	33.5€	17€	1€	16.67€	21€	42€	75€	33€	1€
Cycle Cost Lithium-ion	50€	33€	48€	67€	50€	68€	43.5€	65.5€	87.5€	106.5€
Profit	50.24 €	49 €	50.5€	47.5€	49€	26.74€	30 €	91€	111 €	124€

Table 4.8: The economical results of the cycling tests

Chapter 5

Discussion

The main objective of this thesis was to develop an MPC for a distributed BESS that are supposed to be used for both backup power for a communication antenna (or other communication equipment), and for PFC. The controller should make the plant follow the proposed regulations for PFC, and it should always have enough power in every BESS to drift the communication equipment for a certain time period if the communication equipment for some reason needs to run on battery power instead of using power from the grid. The optimization part of the MPC should try to distribute the total amount of power set to be used for PFC between the sites in order to reduce battery degradation to a minimum. Therefore, in the results chapter, two types of tests were run, where the functionality of the MPC was tested in Sections 4.1 to 4.5. These tests were almost exclusively run with MPC2. This is because the results of the functionality tests are identical for MPC1 and MPC2. This is expected since the only difference between the two is the optimizing part. Whereas MPC1 minimizes the difference between the sum of the power limits and a reference power, and MPC2 minimizes the square root of the cycle-depths given maximum frequency deviation on the prediction horizon.

5.1 Functionality

The acceptance tests conducted in the results chapter shows that the distributed system controlled by the MPC is identical to the test scheme Energinet.dk has proposed.

The control gain for the SOC-compensation part of the controller which was used in the acceptance tests conducted in fig. 4.3, was chosen to be such that the curve from these tests were quite similar to the ones in (Energinet.dk, 2013). As the test in section 4.2 describes, the controller also handles that sites cannot contribute to PFC. This is particularly shown in the third plot in fig. 4.4 where it is shown that the total plant power output is the same over the whole simulation.

If this scheme is to be implemented in a real system, it is crucial that every site receives the new limits synchronously. If not, a scenario where one site receives and starts to use a new limit before another one might occur, and this may result in the plant delivering a wrong amount of power. Delivering too much power is also bad, since this is expensive. This might also be the problem if a site suddenly no longer can participate in PFC. Imagine the scenario where a site gets a new limit from the MPC, and one second later, for some reason, the power in the battery is needed to run the communication load. It sends some kind of message to the MPC that it is unavailable. However, if the MPC is only updated every 10th second, there will be some time period where the plant are not able to deliver enough power. This results in a breach in the agreement between the plant operator and the TSO, and should be avoided. One solution could be that such an event triggered a new solution from the MPC, but due to slow communication between the centralized controller and the distributed BESSs and the runtime of the MPC, this solution will probably not solve the problem.

The maximum capacity test performed in section 4.5, shows that the plant can guarantee the entire inverter-capacity plus to be available for Δf up-regulation. Meaning that this plant may deliver 160kW if all 20 sites have inverters installed. On the other hand, for Δf down-regulation, only the sites with a lithium-ion battery can guarantee that they're always available for down-regulation since it is very unlikely they will be fully charged. The lead acid batteries on the other hand, are often fully charged, hence they cannot always guarantee that they can contribute to Δf down-regulation. Since all sites have rectifiers, this capacity becomes 80kW for the set-up used to produce the results. The size of the plant used in this simulation then, is not large enough by itself to participate in PFC. According to Energinet.dk, a minimum of a symmetrical 1MW is necessary to be accepted. However, it is possible to use this as an auxiliary plant in addition to a designated PFC plant. For down-regulation, it is also possible to use e.g.

heating equipment or other energy demanding plants. In order to serve 1MW down regulation, 250 sites are needed if the rectifier capacity at each site is 8kW. If 16kW is used, the number of sites may be reduced to 125. The runtime of the MPC during simulations varies usually between 0.01 and 0.02 seconds per iteration for 20 sites, hence it can run on a frequency of about $50Hz-100Hz$. Since this is just a QP-problem with linear constraints, there is no reason to believe that the runtime will increase significantly with a larger number of sites added.

The tests in section 4.3 shows that the MPC have some problems keeping the plant inside its boundaries. Therefore, most tests are run with saturated integrators on the battery level such that if power is applied to a fully charged battery, the integrator ignores this power, and leaves the SOC at fully charged such that the battery level does not rise above maximum battery level. The power used for charging a fully charged battery is then ignored. This can be done because the power added to a full battery in these simulations is so small that it is considered negligible. The reason the MPC does not manage to keep the constraints are probably small model inaccuracies or inaccuracies in the solution of the ODE solver used in the simulation. However, although the first is more intuitive, the same thing happens when the plant replacement model and the prediction model in the MPC are exactly the same. Another possibility is that the discretization of the prediction model in the MPC is inaccurate. It is at least shown in fig. 4.5 that the solutions given by the MPC itself never casues the predicted SOCs to break the constraints given an initial start value less than or equal to one. To discretize the prediction model, Euler is used since it is a first order system. However, the entire plant consists of first order differential equations, which means that Simulink could also use Euler to get the correct result. However, running the simulations with the Euler discretization as the ODE solver gives the same result. In order to run this test, slack variables were added to the state of charge constraint in eqs. (3.6h) and (3.6i). This is a physical constraint that never can or will be broken. Adding slack variables to this is not something that should be done, since it is a hard constraint. This means that without the slack variables implemented in these constraints, no solution to the optimization problem can be found because the MPC will receive an initial SOC which is larger than 1, hence the QP solver cannot find a feasible starting point. So in order to illustrate this problem, adding slack variables was necessary. This problem does not affect the degra-

dation tests, since the frequency deviations in those tests are much smaller than in the acceptance test.

5.2 Implementation of the MPC

Implementing an MPC is often just installation of software to already existing infrastructure, which is partially the case in this thesis. On site, all the equipment needed is already installed, except the inverters, which is needed in order to deliver Δf up-regulation. There are also a centralized surveillance system with two-way communication to each site. Some kind of controller is needed anyway, and MPC is a proven technology.

5.3 Degradation Models

There are two types of degradation models used in this thesis. One, that counts the cycles and states that when a certain number of cycles is reached, the battery has to be replaced, and one more advanced part physical part heuristic models. The upside with the cycle counting is that they are easy to implement and easy to understand and battery manufacturers usually states how many cycles their batteries can endure. The downside with those models is that they do not consider other factors such as time, temperature and cycle depth which are important factors for battery degradation. However, in the implementations of the physical battery degradation models in sections 3.2.1 and 3.2.2 some assumptions are made, e.g in the lead-acid degradation model, corrosion is neglected, and the model contains singularities in eqs. (2.16b) and (2.18) where the output is divided with I, which can be dealt with by saying that f_{acid} and f_I is equal to zero when I is equal to zero. However, it is difficult to determine where the limit should be, since when I is close to zero, f_{acid} and f_I are very large. Although it is obvious that for small currents, these effects are large. The question is, how large. So the implementations of the physical battery degradation models may be a bit inaccurate. This is why they are not used for the economical analysis. However, they are believed to show trends in the charging, e.g. the degradation seems to increase with the amount of power cycled through like in fig. 4.10. They are therefore trusted enough

to verify if a controller works better than another controller.

5.4 Ecomomic potential

There seem to be an economic potential in using a distributed BESS for PFC. At least with a larger system than the one used in the simulations in chapter 4. However, with the cycling degradation model, both the profit and cycling cost is linearly scalable.In the simulations conducted, it was the test where the lead acid batteries was hardly used which turned out to be the most profitable. The reason for this is that even though lithium-ion batteries are more expensive to buy, they last longer meaning that one cycle in a lithium-ion battery is cheaper than one cycle in a lead-acid battery according to eq. (3.4). In test 10 in table 4.8, the active sites are the ten sites that contains lithium-ion batteries. It will also be recommended to install double rectifier and inverter capacity on each site, since even though the power capacities double, the cycle cost does not seem to do that. This means that for a system with only lithium-ion 100 sites that delivers $1.4MW$, the revenue would be about 1250€ for the simulation period of 500000 seconds. Lead-acid sites are also profitable in this scheme, so including old sites in PFC is also recommended.

5.5 MPC performance

The optimization in MPC2 is based on a worst case scenario where the limits are chosen to be the limits that minimizes the sum of the squares of the battery cycle depth on each site. However, as can be seen by the tests in table 4.3 it performs worse than MPC1 which makes a more or less coincidental power distribution. What is particularly interesting is that in the test with the frequency measurements from Denmark the sum of the squares of the DOD at each site at each time-step is about twice as big for MPC2 than for MPC1. Since the MPC2 object function is based on a worst-case scenario, it should perform better with 10 times as large frequency deviations. However, in that test, the sum was about three times larger for MPC2 than MPC1. This then points to either that the prediction model for the DOD is wrong, or that the assumption that the maximum frequency deviation last over the whole prediction horizon is a bad assumption. From

fig. 4.10 it can at least be seen that it is a wrong assumption.

Judging the controllers by the degradation results from the physical models, it seems like the perform about equally. However, MPC2 holds the benefit that it can be tuned. From the degradation models it can actually seem like the MPC2 with no weights on the lead-acid battery might be the best controller. Since table 4.6 shows a nominal degradation result, it may seem like it is the cheapest since lead-acid batteries are cheaper than lithium-ion batteries per kWh. From tests 6 and 7 it might also seem like MPC2 handles a higher variance in the batteries better than MPC1.

The best economical result is that of test 10 in table 4.7 which gives a profit of 125€. However, the reason for this is that it does not use the lead-acid batteries at all, which according to the cycling model is more expensive to cycle. However, both the degradation models used shows that the differences on the controllers when it comes to degradation are very small.

Chapter 6

Conclusion and Further Works

6.1 Conclusion

Some aspects of the MPC works, and it will make the plant follow the regulations given by the danish TSO. However, MPC2, which is supposed to minimize battery degradation, does not perform better than the naive approach in MPC1. The reason for this is that minimizing x_{DOD}^2 was probably the wrong choice. This is thought to be the problem since, even though the degradation results are pretty similar, the results in table 4.3 shows that the sum of the squares of the cycle depths are twice as large for MPC2. The fact that MPC2 actually performs worse than MPC1 when it comes to distribute the limits evenly among the batteries also shows that the calculating the limits that are optimal if there is a maximal frequency deviation throughout the prediction horizon is also wrong. However, it was also the only realistic objective to be used in an MPC in order to reduce battery degradation. Since the only other thing that is possible to control that wears batteries is the number of cycles. However, doing this with an MPC is not straight forward. The advantage with MPC2 is that it is possible to decide which batteries should be used the most. And as a controller for a distributed BESS, it works well. The only downside is the problem with the controller not being able to keep the constraints. However, this is probably caused by some small inaccuracies. But a more robust design is needed.

The controller is simple to implement, assuming that the infrastructure is in place.

Which means the only installation cost is the cost of the software design and software installation. If new sites are built, it is recommended that Lithium-ion batteries are installed. These batteries are more expensive, but the cycling cost is lower than for lead-acid making it a valuable investment.

6.2 Further works

The first that needs to be done is to implement a mechanism on each site that makes sure that fully charged batteries does not get over-charged. This can be done as easily as multiplying P_{PFC} with a boolean that is false when the battery is full and Δf is positive. $P_{\text{SOC,compensation}}$ is always zero when the battery is full anyway. Some other MPC approaches could be tried. Along with more computing power and fast communication between the sites and the centralized control-center, an MPC that controls the power-flow through the rectifier/inverter directly. This was tried in (Hestdal, 2013), however the conclusion was that it run too slow. Another MPC approach which should be explored is a version of MPC1, with an addition in the objective function which makes sure all sites are used. This could be as simple as:

$$u_{\text{min}}^T Q_1 u_{\text{min}} + u_{\text{max}}^T Q_2 u_{\text{max}} \tag{6.1}$$

This would probably not make an impact on battery degradation, but would make it possible to tune the MPC to favour some sites more than others.

It is also unclear which regulations that applies for PFC sites that also serves auxiliary services such as backup-power for communication equipment. This needs to be investigated further.

Appendix A

MATLAB Code

A.1 MPC1

```
1
2  %limits is the vector which contains u_max and u_min, SOC is a ...
       vector with SOC from all sites, load is the site load on each ...
       site, t is the simulation time and participate_signals is the ...
       Z - vector.
3
4  function limits = MPC1(SOC,load,~,t,~,participate_signals)
5
6
7  %declaring persistent variables. Declaring the Controller and the ...
       number of sites N to be persisten variables.
8  persistent Controller
9  persistent N
10
11 % The first iteration of the loop defines the control problem
12 if t == 0
13
14      %N number of sites, L is the prediction horizon in seconds
15      N = 20;
16      L = 20;
17
```

```
%defining the MVs
    u_min = sdpvar(repmat(N,1,1),repmat(1,1,1));
    u_max = sdpvar(repmat(N,1,1),repmat(1,1,1));

%defining the CVs

    x_SOC_max = sdpvar(repmat(N,1,L+1),repmat(1,1,L+1));

    x_SOC_min = sdpvar(repmat(N,1,L+1),repmat(1,1,L+1));


%defining the DVs
    site_load = sdpvar(repmat(N,1,1),repmat(1,1,1));
    participate = sdpvar(repmat(N,1,1),repmat(1,1,1));

%defining the battery capacities

        capacity =[ 207360;
                    224640;
                    172800;
                    207360;
                    190080;
                    155520;
                    241920;
                    259200;
                    224640;
                    190080;
                    207360;
                    224640;
                    172800;
                    207360;
                    190080;
                    155520;
                    241920;
                    259200;
                    224640;
                    190080;];

    %defining charge_constant

```

```
58      charge_constant = 0.004.*capacity;
59
60       %defining SOC limits and reference
61
62       SOC_min_lim = 0.4;
63       SOC_max_lim = 1;
64       SOC_ref = [ones(1,N/2),0.7*ones(1,N/2)];
65
66      %Defining rectifier and inverter capacities
67
68       power_electronics_capacity_max = 8*ones(N,1);
69       power_electronics_capacity_max(1) = 0;
70       power_electronics_capacity_max(5) = 0;
71       power_electronics_capacity_max(11) = 0;
72       power_electronics_capacity_max(15) = 0;
73
74       power_electronics_capacity_min = 8*ones(N,1);
75
76
77      %Defining P_PFC bot for negative and positive \Delta f
78       committed_power_max = 70;
79       committed_power_min = 70;
80
81      %Declaring the constraints and objective variables
82       constraints = [];
83       objective = 0;
84
85       %loops over each time-step k for each site i
86       for k = 1:L
87
88           %defining the objective function
89           objective = (participate'*u_max - committed_power_max)^2 + ...
                (participate'*u_min- sum(site_load) - ...
                committed_power_min)^2;
90
91           for i = 1:N
92
93           %defining the constraints
94
95           %adding the plant model constraints
```

```
96              constraints = [constraints, x_SOC_max{k+1}(i) == ...
                    x_SOC_max{k}(i)*(1-1/charge_constant(i)) + ...
                    SOC_ref(i)/charge_constant(i) - u_max(i)/capacity(i)];
97              constraints = [constraints, x_SOC_min{k+1}(i) == ...
                    x_SOC_min{k}(i)*(1-1/charge_constant(i)) + ...
                    SOC_ref(i)/charge_constant(i) + u_min(i)/capacity(i)];
98
99          %adding the power ouuput from each site as constraints
100             constraints = [constraints, 0 <= u_max(i) <= ...
                    power_electronics_capacity_max(i) + site_load(i)];
101             constraints = [constraints, 0 <= u_min(i) <= ...
                    power_electronics_capacity_min(i) - site_load(i)];
102         end
103
104     end
105
106
107     %Adding constraints on the state of charge
108
109     constraints = [constraints, SOC_min_lim <= [x_SOC_max{:}] <= ...
            SOC_max_lim];
110     constraints = [constraints, SOC_min_lim <= [x_SOC_min{:}] <= ...
            SOC_max_lim];
111
112
113
114   %Defines the Controller by using the optimizer command
115     Controller = ...
            optimizer(constraints,objective,sdpsettings('solver','gurobi','verbose',2),x_S
116
117
118   %Solve the optimization problem given the Cvs and Dvs in the ...
        first iteration
119     limits = Controller{{SOC,SOC,load,participate_signals}};
120
121 else
122   %Solve the optimization problem for each iteration where t >= 0
123     limits = Controller{{SOC,SOC,load,participate_signals}};
124
125 end
```

A.2 MPC2

```
1
2  %limits is the vector which contains u_max and u_min, SOC is a ...
       vector with SOC from all sites, load is the site load on each ...
       site, t is the simulation time and participate_signals is the ...
       Z - vector.
3
4  function limits = MPC2(SOC,load,DOD,t,P_committed,participate_signals)
5
6
7  %declaring persistent variables. Declaring the Controller and the ...
       number of sites N to be persisten variables.
8  persistent Controller
9  persistent N
10
11 % The first iteration of the loop defines the control problem
12 if t == 0
13
14     %N number of sites and L is the prediction horizon
15     N = 20;
16     L = 20;
17
18     %defining the MVs
19
20     u_min = sdpvar(repmat(N,1,1),repmat(1,1,1));
21     u_max = sdpvar(repmat(N,1,1),repmat(1,1,1));
22
23     %defining the CVs
24     x_DOD_li_max = sdpvar(repmat(2*N,1,L+1),repmat(1,1,L+1));
25     x_DOD_li_min = sdpvar(repmat(2*N,1,L+1),repmat(1,1,L+1));
26
27     x_SOC_max = sdpvar(repmat(N,1,L+1),repmat(1,1,L+1));
28
29     x_SOC_min = sdpvar(repmat(N,1,L+1),repmat(1,1,L+1));
```

```
30
31      %defining the Z vector
32      participate = sdpvar(repmat(N,1,1),repmat(1,1,1));
33
34      %Defining P_PFC bot for negative and positive \Delta f
35      committed_power_max = 70;
36      committed_power_min = 70;
37
38      %Defining slack variables fpr the power constraint
39      sdpvar power_slack1
40      sdpvar power_slack2
41
42      %declaring the site load DV
43      site_load = sdpvar(repmat(N,1,1),repmat(1,1,1));
44
45
46
47
48
49  %defining the battery capacities
50          capacity =[ 207360;
51                      224640;
52                      172800;
53                      207360;
54                      190080;
55                      155520;
56                      241920;
57                      259200;
58                      224640;
59                      190080;
60                      207360;
61                      224640;
62                      172800;
63                      207360;
64                      190080;
65                      155520;
66                      241920;
67                      259200;
68                      224640;
69                      190080;];
```

```
70
71      %defining the charge constant for the SOC compensation
72      charge_constant = 0.004.*capacity;
73
74      %defining rectifier/inverter capacities
75      power_electronics_capacity_max = 8*ones(N,1);
76
77
78      power_electronics_capacity_min = 8*ones(N,1);
79
80
81      %Matrices for the DOD model
82      Bd = [1;0];
83      Bc = [0;1];
84
85      Ad = [1 0;
86            0 0;];
87
88      Ac = [0 0;
89           0 1;];
90
91      limits and references for the state of charge
92      SOC_min_lim = 0.4;
93      SOC_max_lim = 1;
94      SOC_ref = [1 1 1 1 1 1 1 1 1 1 0.7 0.7 0.7 0.7 0.7 0.7 0.7 ...
            0.7 0.7]';
95
96      %Weight matrices
97      Q1 = diag([ones(1,N),ones(1,N)]);
98      Q2 = diag([ones(1,N),ones(1,N)]);
99
100
101     %constraints and objective function variables
102     constraints = [];
103     objective = 0;
104
105
106     looping over discrete time k and number of sites i
107     for k = 1:L
108         %defining the objective function
```

```
109         objective = objective + ...
               x_DOD_li_max{k}'*Q1*x_DOD_li_max{k} + ...
               x_DOD_li_min{k}'*Q2*x_DOD_li_min{k};
110
111         for i = 1:N
112
113         %cosntraints for the DOD model
114             constraints = [constraints, ...
                   x_DOD_li_max{k+1}(2*i-1:2*i) == ...
                   Ad*x_DOD_li_max{k}(2*i-1:2*i) + Bd.*(((SOC_ref(i) ...
                   - x_SOC_max{k}(i))/charge_constant(i)) + ...
                   u_max(i)/capacity(i))];
115             constraints = [constraints, ...
                   x_DOD_li_min{k+1}(2*i-1:2*i) == ...
                   Ac*x_DOD_li_min{k}(2*i-1:2*i) + ...
                   Bc.*(((x_SOC_min{k}(i) - ...
                   SOC_ref(i))/charge_constant(i)) + ...
                   u_min(i)/capacity(i))];
116
117
118           %constraints describing the SOC model
119             constraints = [constraints, x_SOC_max{k+1}(i) == ...
                   x_SOC_max{k}(i) + ...
                   (SOC_ref(i)-x_SOC_max{k}(i))/charge_constant(i) - ...
                   u_max(i)/capacity(i)];
120             constraints = [constraints, x_SOC_min{k+1}(i) == ...
                   x_SOC_min{k}(i) + ...
                   (SOC_ref(i)-x_SOC_min{k}(i))/charge_constant(i) + ...
                   u_min(i)/capacity(i)];
121
122           %constraints for the power flow at each site
123             constraints = [constraints, 0 <= u_max(i) <= ...
                   participate(i)*(power_electronics_capacity_max(i) ...
                   + site_load(i))];
124             constraints = [constraints, 0 <= u_min(i) <= ...
                   participate(i)*(power_electronics_capacity_min(i) ...
                   - site_load(i))];
125
126
127         end
```

```
128
129     end
130
131
132     %adding the slack variables for P_PFC to the objective function
133     objective = objective + 10e5*power_slack1 + 10e5*power_slack2;
134
135     %Box constraints for the state of charge
136     constraints = [constraints, SOC_min_lim <= [x_SOC_max{:}] <= 1 ];
137     constraints = [constraints, SOC_min_lim <= [x_SOC_min{:}] <= 1 ];
138
139
140
141     %constraints for ensuring correct P_PFC. With slack variables
142     constraints = [constraints, participate'*u_max  == ...
            committed_power_max - power_slack1];
143     constraints = [constraints, participate'*u_min  == ...
            committed_power_min - power_slack2];
144
145     %limits for the slack variables. For computational speed.
146     constraints = [constraints, 0 <= power_slack1 <= ...
            committed_power_max];
147     constraints = [constraints, 0 <= power_slack2 <= ...
            committed_power_min];
148
149     %defining the controller by using YALMIPS optimizer command
150     Controller = ...
            optimizer(constraints,objective,sdpsettings('solver','gurobi','verbose',2),{x_
151
152      %Solve the optimization problem given the Cvs and Dvs in the ...
            first iteration
153     limits = Controller{{DOD,DOD,SOC,SOC,load,participate_signals}};
154
155 else
156     %Solve the optimization problem given CVs and DVs for t > 0
157     limits = Controller{{DOD,DOD,SOC,SOC,load,participate_signals}};
158
159 end
```

A.3 Lead-acid Degradation Model

A.3.1 Bad Charges Count

```
%increase_new is a variable that states if n should be increased ...
    or not in the next iteration
%SOC_prev_new is the previous SOC_new in the next iteration
%SOC_new  is the current SOC
%increase is a variable that states if n should be increased or not
%SOC_prev_prev is SOC(k-2)
%SOC_prev  is SOC(k-1)
%n_prev is n(k-1)
%SOC is the state of charge
function [increase_new,SOC_prev_new,SOC_new,n]  = ...
    fcn(increase,SOC_prev_prev,SOC_prev,n_prev,SOC)



SOC_lim = 0.95;
SOC_ref = 0.95;

%n should only be increased  if SOC is larger than 0.95
if SOC < 0.95
    increase_new = 1;
else
    increase_new = increase;
end


if SOC >= 0.9999
    n = 0;
elseif (SOC_prev_prev <= SOC_prev) && (SOC <= SOC_prev) && (SOC >= ...
    SOC_lim) && (increase == 1) %checks if SOC_prev is a ...
    maximum-point and if n can be increased
    n = n_prev + (0.0025-(SOC_ref-SOC_prev)^2)/0.0025; %increases n
    increase_new = 0;
else
    n = n_prev;   %does nothing
```

```
31 end
32
33 SOC_prev_new = SOC_prev;
34
35 SOC_new = SOC;
```

A.3.2 Current Factor

```
1  function f_I_n  = fcn(n,I)
2
3  I_10 = 5.4;
4
5
6  %To avoid singularities:
7  if I < -0.00005
8
9      f_I  = (nthroot(I_10/I,3)^2);
10
11     f_I_n = f_I*nthroot(exp(n/3.6),3);
12
13 else
14     f_I_n = 0;
15 end
```

A.3.3 SOC min calculation

```
1  %calculates the lowest SOC since last full charge
2  function [SOC_min,t_0] = fcn(SOC,SOC_min_prev,t_0_prev,t)
3
4  if (SOC <= SOC_min_prev) || (SOC >= 0.95)
5      SOC_min = SOC;
6  else
7      SOC_min = SOC_min_prev;
8  end
9
```

```
if SOC >= 1
    t_0 = t;
else
    t_0 = t_0_prev;
end
```

A.3.4 Voltage calculation

```

%Calculates the cell voltage
function U = fcn(I,SOC)


U_0 = 2.1; %Open circuit voltage
g = 0.076; %Gradient of change in OCV with SOC
C_N = 54*60*60; %Nominal capacity
M_c = 0.888; %Resistance representing charge-transfer process ...
    which depends on SOC (charging)
M_d = 0.0464; % Resistance representing charge-transfer process ...
    which depends on SOC (discharging)
rho_c = 0.42; %Effective internal resistance (charging)
rho_d = 0.699; %Effective internal resistance (discharging)
C_c = 1.001; %Normalized capacity of battery (charging)
C_d = 1.75; %Normalized capacity of battery (discharging)


DOD = 1-SOC;

if I <= 0

    U = U_0 -g*DOD + rho_d*I/C_N + (rho_d*M_d*I/C_N)*DOD/(C_d-DOD);

else

    U = U_0 -g*DOD + rho_c*I/C_N + (rho_c*M_c*I/C_N)*SOC/(C_c-SOC);

end
```

A.3.5 Gassing current

```
%Calculates the gassing current
function I_gas = fcn(U,T)

C_N = 54;  %Cellc capacity
I_gas0 = 20e-3; %Normalized gassing current at T_gas0 and U_gas0
T_gas0 = 298; %Nominal temperature for gassing
U_gas0 = 2.23; %Nominal voltage for gassing
c_u = 11; %Voltage coefficient
c_T = 0.06; %Temperature coefficient



I_gas = (C_N/100)*I_gas0*exp(c_u*(U-U_gas0) + c_T*(T-T_gas0));
```

A.3.6 SOC Stress Factor

```
function f_SOC  = fcn(f_I_n,SOC_min,t_0,t)

c_SOC_0 = 6.614e-5; %Cosntant slope for SOC factor

c_SOC_min = 3.307e-3; Impact of the minimum SOC on the SOC factor

delta_t_SOC = (t-t_0)/(3600);

f_SOC = 1 + (c_SOC_0 + c_SOC_min*(1-SOC_min))*f_I_n*delta_t_SOC;
```

A.3.7 Stratification

```
function f_plus = fcn(f_stratification,I,SOC_min)

c_plus = 1/30;
```

```
I_ref = 5.4;

f_plus = c_plus*(1-SOC_min)*exp(-3*f_stratification)*abs(I)/I_ref;

%%%%%%%%%%%%%%%%%%%%%%%%%%%%%%%%%%%%%%%%%%%%%%%%%%%%%%%%%%%%%%%%%%%%%%%%%%%%

function f_minus_diffusion = fcn(f_stratification,T)

z = 30;  %Battery height (cm)
D = 10^(-9); %Diffusion constant for sulfuric acid

f_minus_diffusion = (8*D/z^2)*f_stratification*2^((T-293)/10);

%%%%%%%%%%%%%%%%%%%%%%%%%%%%%%%%%%%%%%%%%%%%%%%%%%%%%%%%%%%%%%%%%%%%%%%%%%%%

function f_minus_gassing = fcn(I_gas,T,U)

U_ref = 2.5;
c_minus = 0.1;
C_N = 54*60*60;
c_T = 0.06;
I_gas0 = 20;
T_gas0 = 298;
c_u  = 11;


if U >= 2.3
    f_minus_gassing = ...
       c_minus*sqrt(100/C_N)*(I_gas/I_gas0)*exp(c_u*(U-U_ref) + ...
       c_T*(T-T_gas0));
else
    f_minus_gassing = 0;
end


%%%%%%%%%%%%%%%%%%%%%%%%%%%%%%%%%%%%%%%%%%%%%%%%%%%%%%%%%%%%%%%%%%%%%%%%%%%%

function f_acid = fcn(I,f_stratification)

C_N = 54*60*60;
```

```
I_10 = 5.4;

if (I >= 0.00005) || (I <= -0.00005)
    f_acid = 1 + f_stratification*sqrt(I_10/abs(I));
else
    f_acid = 1;
end

%%%%%%%%%%%%%%%%%%%%%%%%%%%%%%%%%%%%%%%%%%%%%%%%%%%%%%%%%%%%%%%%%%%%%%%%%%
```

A.3.8 Weighted Cycle Count

```
function z_w_dot = Z_W_dot(f_SOC,I,f_acid)

C_N = 54*60*60;

if I <= 0
    z_w_dot = abs(I)*f_SOC*f_acid/C_N;
else
    z_w_dot = 0;
end
```

A.3.9 Degradation Calculation

```
function c_deg = C_deg(Z_W)

c_z = 5;
c_deg_limit = 0.8;
Z_IEC = 600;

c_deg = c_deg_limit*exp(-c_z*(1-Z_W/(1.6*Z_IEC)));
```

A.3.10 DOD Calculation

```
%Battery current(the current has been divided with the battery ...
    capacity before it is taken in) and current DOD as input
function DOD_new = DOD_fcn(DOD,current)


%Matrices for DOD model
Ad = [1 0;
      0 0];

Ac = [0 0;
      0 1];

Bd = [1;0];

Bc = [0;1];

%Calculates the new DOD using the DOD model
if current < 0
    DOD_new = Ad*DOD - Bd.*(current);
elseif current > 0
    DOD_new = Ac*DOD + Bc.*(current);
else
    DOD_new = [0;0];
end
```

A.4 Lithium-ion Degradation Model

A.4.1 Degradation Model

```
function [squared_voltage_sum,cycling_degradation,capacity]  = ...
    battery_degradation_lithium(squared_voltage_sum_prev,cycling_degradation_prev,t,SO


coder.extrinsic('-sync:on','rms');

%T = 25 degrees celsius in kelvins
```

```
7
8  T = 298.15;
9
10 time_in_days = t/(60*60*24);
11
12 %voltage is the cell voltage as a function of the state of charge
13
14 voltage = 3.3324 + 2.1021*SOC -5.8485*SOC^2 + 8.0326*SOC^3 - ...
       3.4599*SOC^4;
15
16 squared_voltage_sum = voltage^2 + squared_voltage_sum_prev;
17
18 %Converts to Ah
19 Q = abs(current)/(60*60);
20
21 %Calculates RMS voltage
22 quadratic_average_voltage = sqrt(squared_voltage_sum/(t+1));
23
24 % beta_cap and alpha_cap are constants used in the
25 % degradation model.
26
27 beta_cap = 7.348e-3*(quadratic_average_voltage-3.667)^2 + 7.6e-4 + ...
       4.081e-3*sum(abs(DOD));
28
29 alpha_cap = ((7.543*voltage-23.75)*10^6)*exp(-6976/T);
30
31 %calculates the cycling degradation
32 cycling_degradation = cycling_degradation_prev + beta_cap*sqrt(Q);
33
34 %Calcultes new capacity by subtracting the time degradation and ...
       cycling degradation from 1
35 capacity = 1 -  alpha_cap*time_in_days^0.75 - cycling_degradation;
```

A.4.2 DOD Calculation

```
1  %Battery charge/discharge power, current DOD and battery capacity ...
       as input
```

```
function DOD_new = DOD_fcn(DOD,power,capacity)

%matrices for DOD model
Ad = [1 0;
      0 0];

Ac = [0 0;
      0 1];

Bd = [1;0];

Bc = [0;1];


%Calculates the new DOD using the DOD model
if power <= -0.01
    DOD_new = Ad*DOD - Bd.*(power/capacity);
elseif power >= 0.01
    DOD_new = Ac*DOD + Bc.*(power/capacity);
else
    DOD_new = [0;0];
end
```

Appendix B

Complete set of Plots for one Simulation

The simulation here are run with the battery storages from tables 4.1 and 4.2, and P_{PFC} to be symmetrical 70kW. The rectifier and inverter capacities are 8kW.

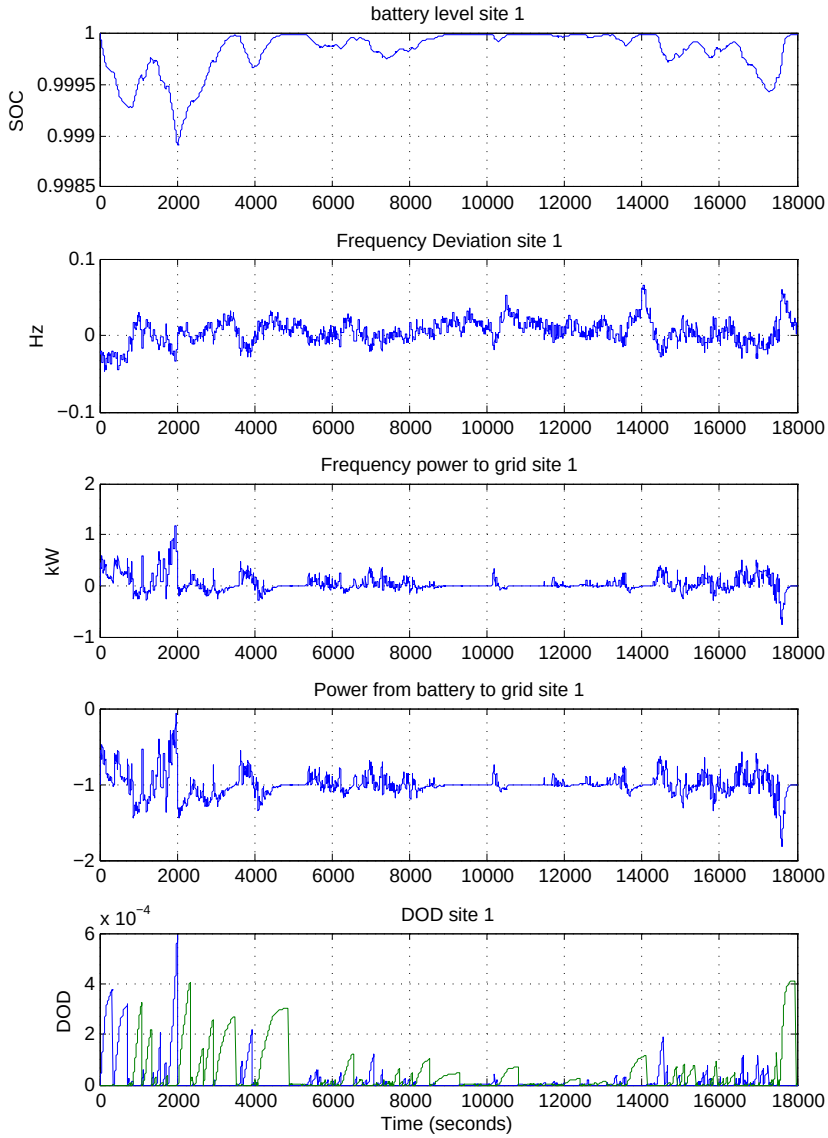

Figure B.1: Simulation plots from test site 1

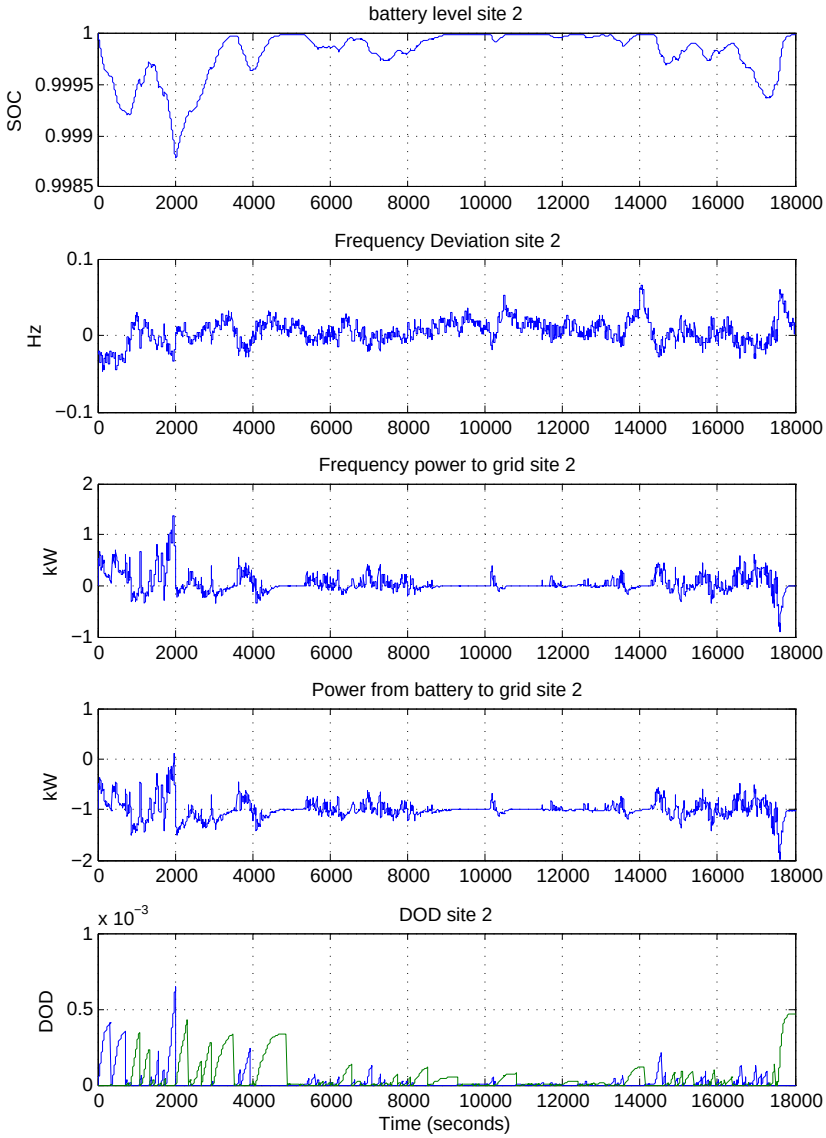

Figure B.2: Simulation plots from test site 2

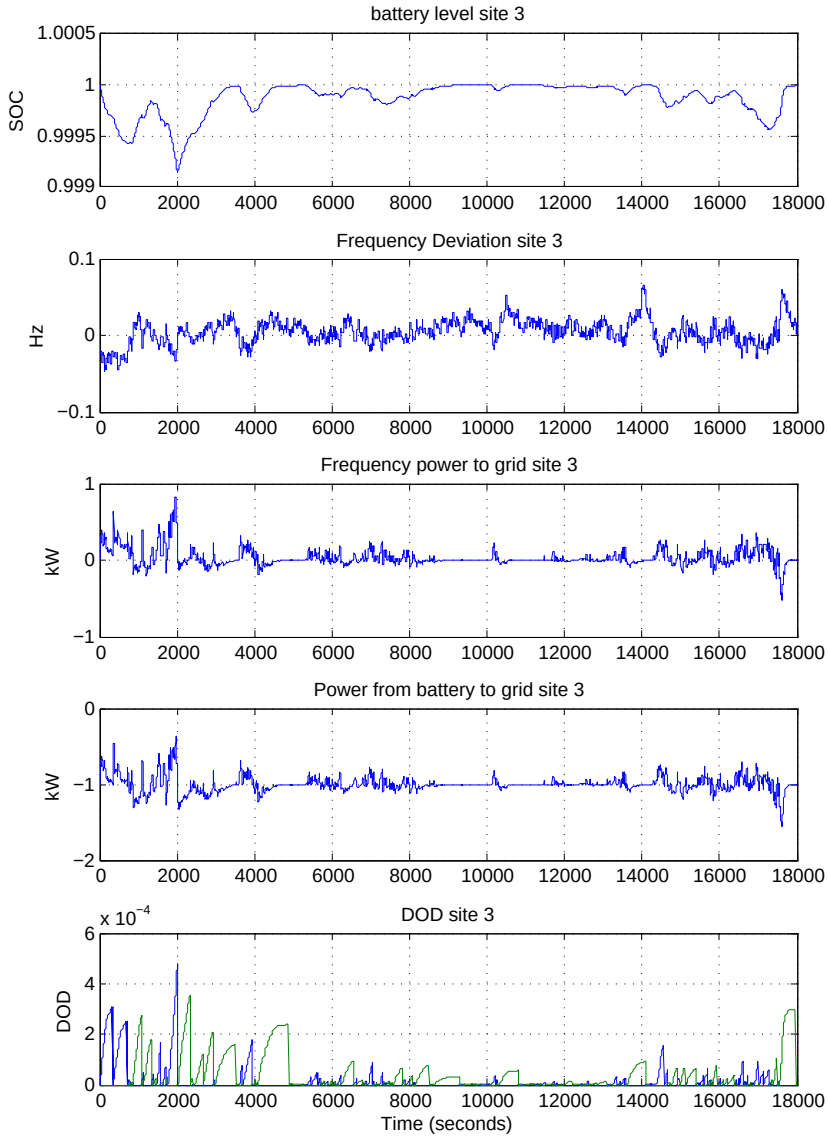

Figure B.3: Simulation plots from test site 3

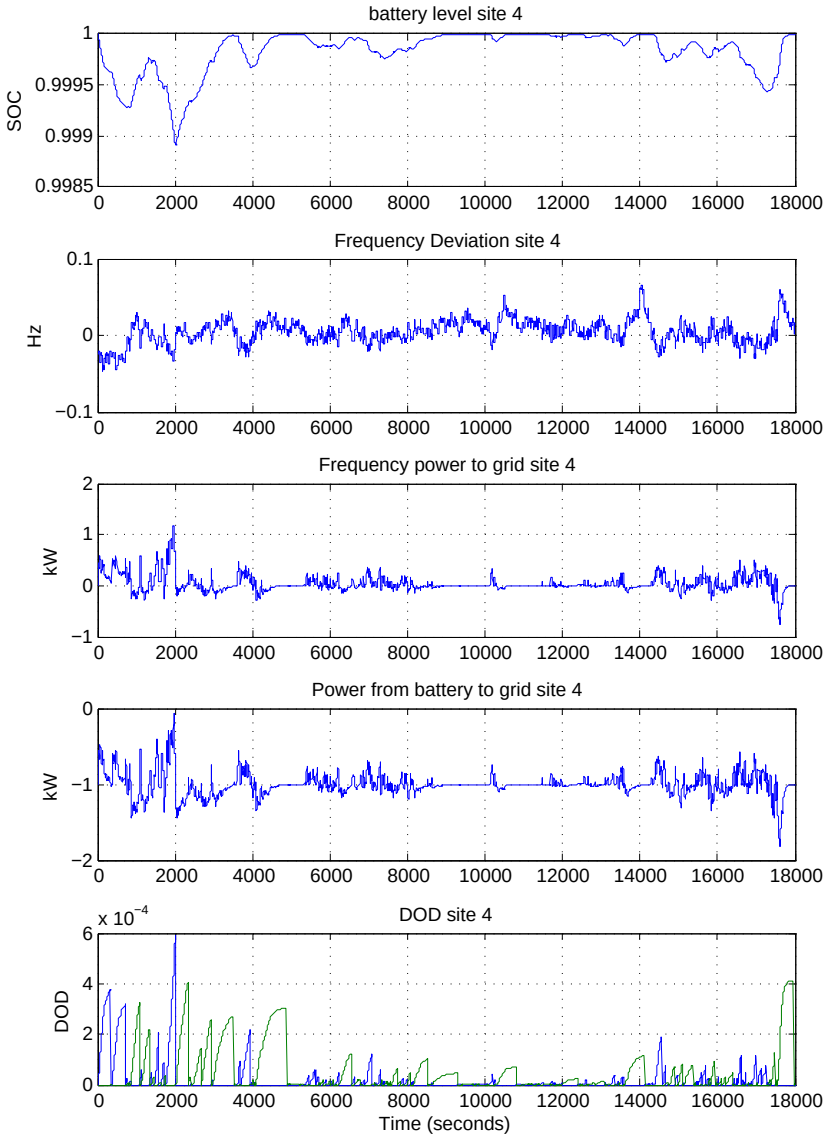

Figure B.4: Simulation plots from test site 4

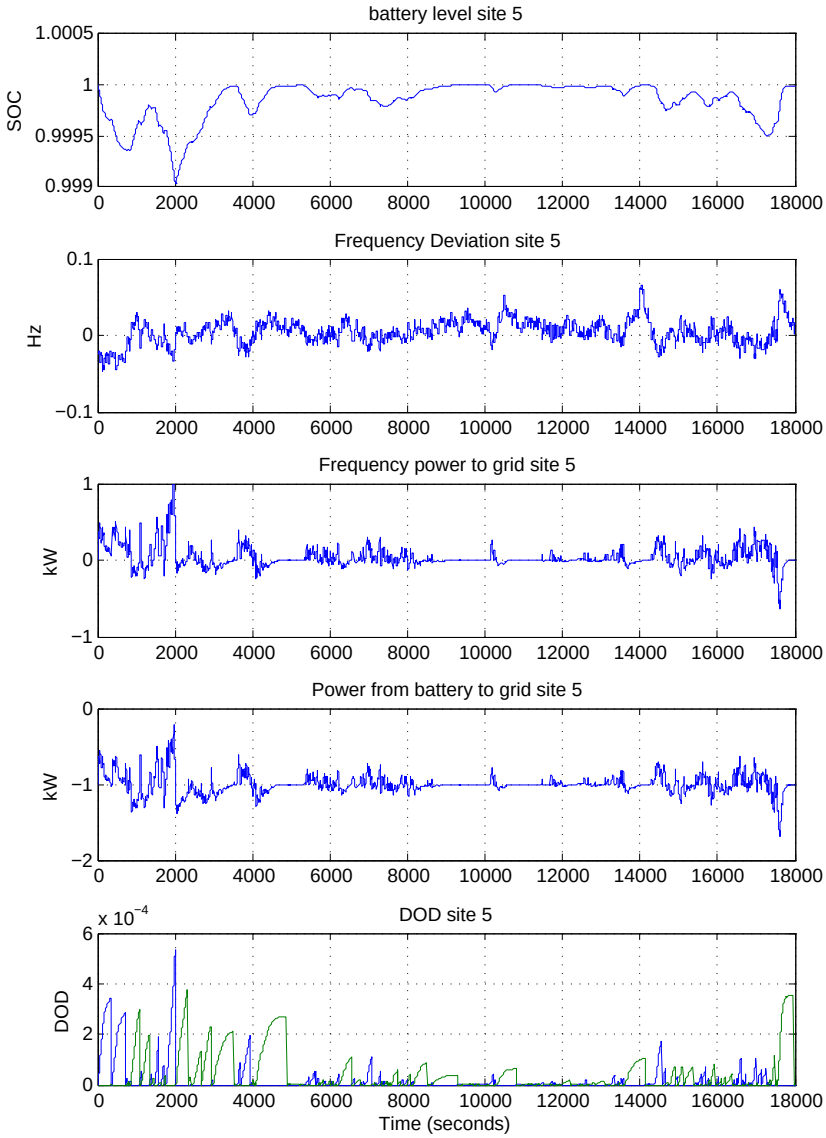

Figure B.5: Simulation plots from test site 5

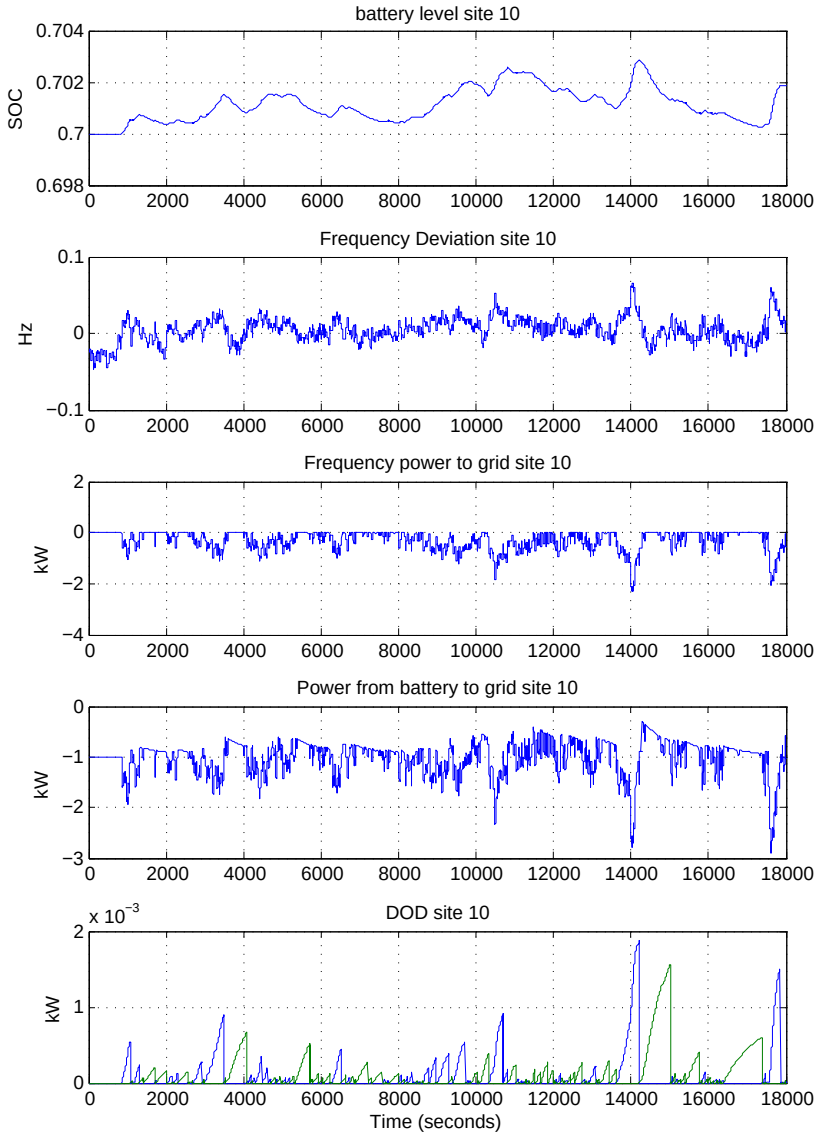

Figure B.6: Simulation plots from test site 10

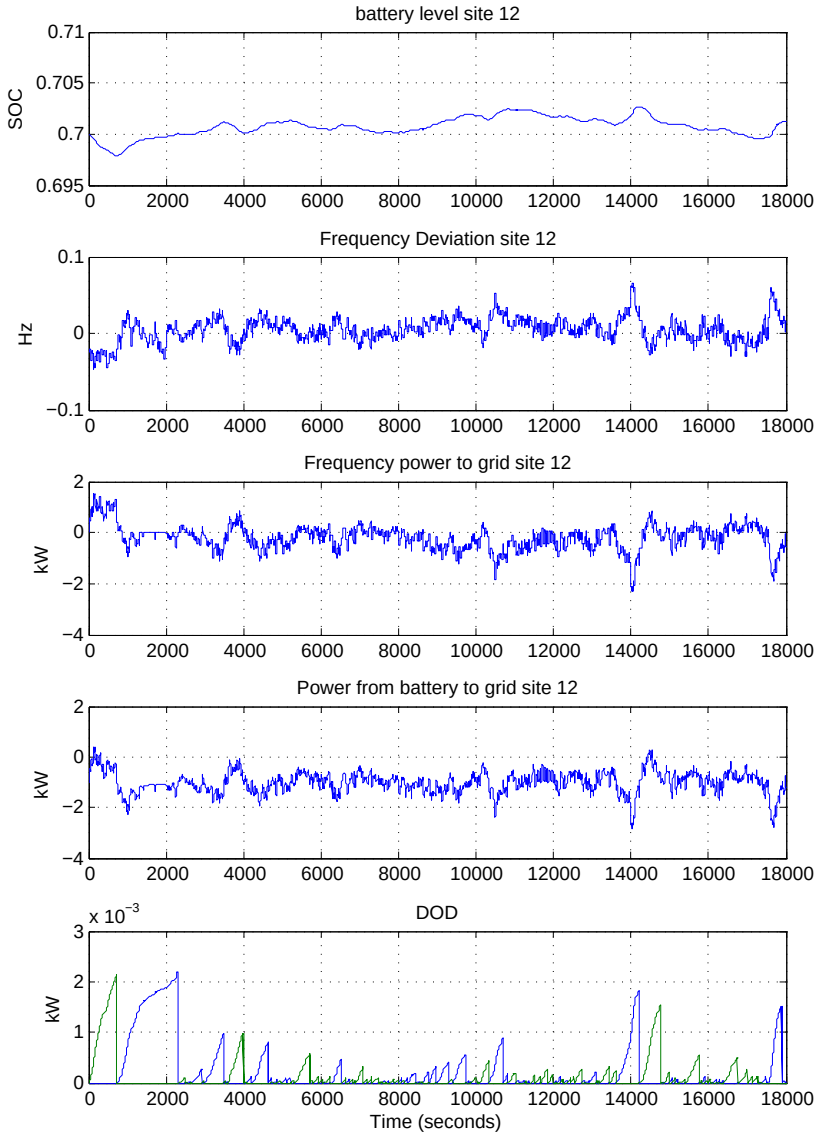

Figure B.7: Simulation plots from test site 11

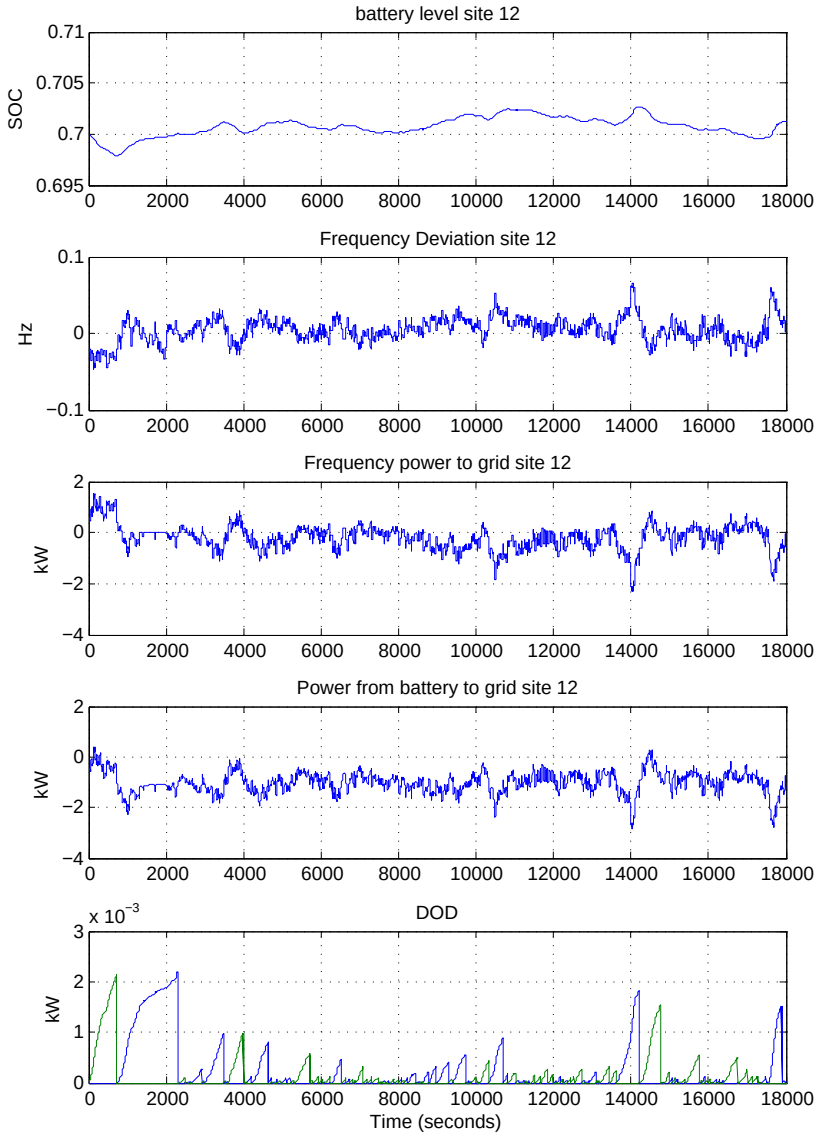

Figure B.8: Simulation plots from test site 12

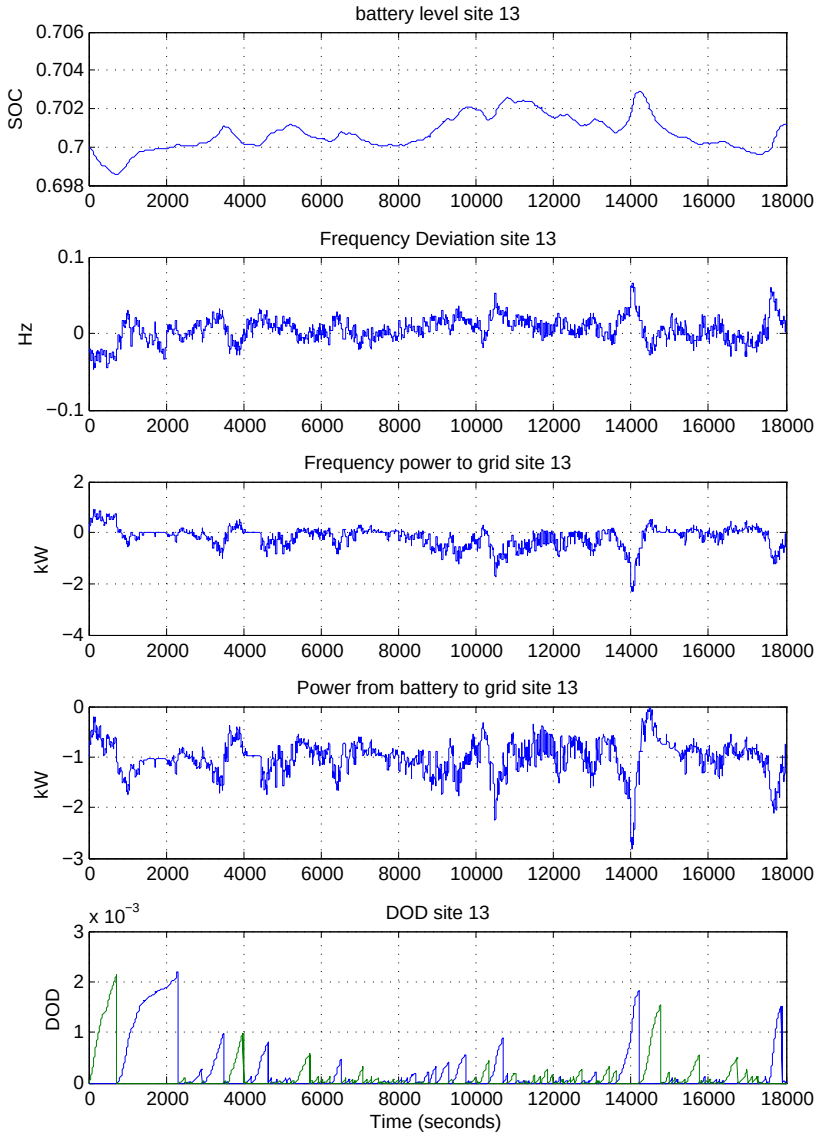

Figure B.9: Simulation plots from test site 13

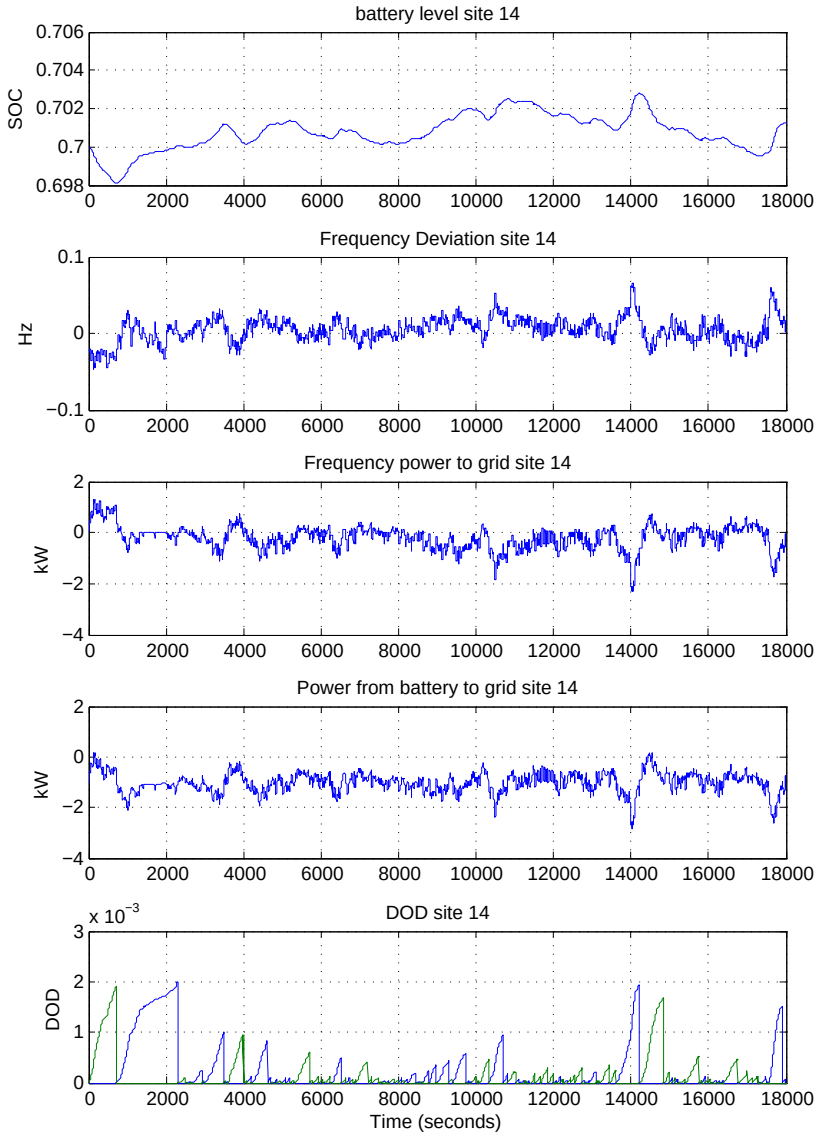

Figure B.10: Simulation plots from test site 14

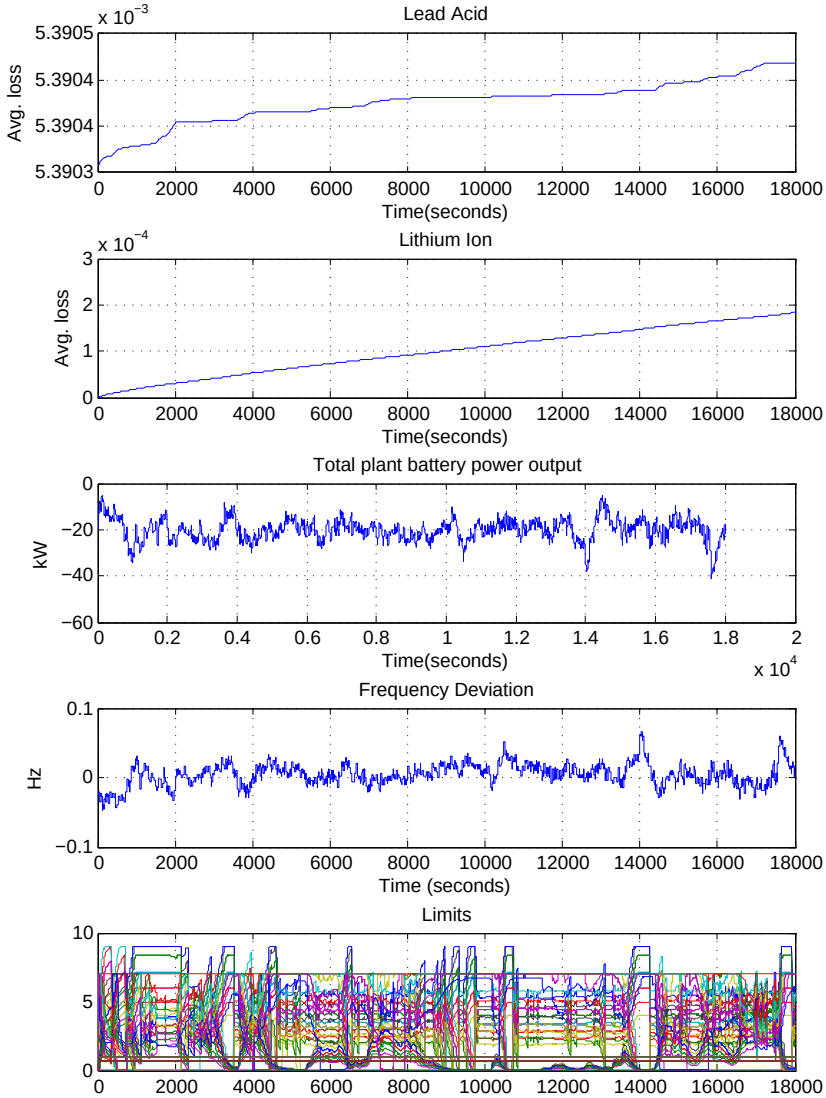

Figure B.11: Plots of the total power output, battery degradation and the calculated limits from the MPC

Bibliography

Water loss, acid stratification and surface charge. http://batteryuniversity.com/learn/article/water_loss_acid_stratification_and_surface_charge.

Ecker, M., Nieto, N., Käbitz, S., Schmalstieg, J., Blanke, H., Warnecke, A., and Sauer, D. U. (2013). Calendar and cycle life study of li(nimnco)o_2 based 18650 lithium-ion batteries. *Journal of Power Sources 248 (2014) 839-851*.

Energinet.dk (2013). Batteries as supplier of frequency-controlled reserves.

Ersdal, A. M., Cecîlio, I., Fabozzi, D., Imsland, L., and Thornhill, N. (2013). Power system model predictive frequency control, taking into account inbalance uncertainty.

Foss, B. and Heirung, T. A. N. (2013). Merging optimization and control.

Hestdal, M. R. (2013). The use of model predictive control and distributed energy storages for primary frequency control.

Heussen, K., Koch, S., Ulbig, A., and Andersson, G. (2012). Unified system-level modeling of intermittent renewable energy storage for power system operation. *IEEE Systems Journal Vol. 6, NO.1, MARCH 2012*.

Khalid, M. and Savkin, A. (2010). A model predictive control approach to the problem of wind power smoothing with controlled battery storage. *Renewable Energy 35 (2010) 1520-1526*.

Koller, M., Borsche, T., Ulbig, A., and Andersson, G. (2013). Defining a degradation cost function for optimal control of a battery energy storage system.

Löfberg, J. (2013). Yalmip wiki. http://users.isy.liu.se/johanl/yalmip/.

Schiffer, J., Sauer, D. U., Bindner, H., Cronin, T., Lundsager, P., and Kaiser, R. (2006). Model prediction for ranking lead-acid batteries according to expected lifetime in renewable energy systems and autonomous power-supply systems. *Journal of Power Sources 168(2007)66-78*.

Schmalstieg, J., Käbitz, S., Ecker, M., and Sauer, D. U. (2014). A holistic aging model for li(nimnco)o_2 based 18650 lithium-ion batteries. *Journal of Power Sources(2014)doi:10.1016/j.jpowsour.2014.02.012*.

Teleke, S., Baran, M. E., Bhattacharya, S., and Huang, A. Q. (2010). Optimal control of battery energy storage for wind farm dispatching. *IEEE Transactions on Energy Conversion, Vol. 25, NO.3,September 2010*.

Thorbergsson, E., Knap, V., Swierczynski, M., Stroe, D., and Teodorescu, R. (2013). Primary frequency regulation with li-ion battery based energy storage system - evaluation and comparison of different control strategies.